

Original Article

Cite this article: Petrizzo MR and Gale AS. Planktonic foraminifera document palaeoceanographic changes across the middle Cenomanian carbon-isotope excursion MCE 1: new evidence from the UK chalk. *Geological Magazine* <https://doi.org/10.1017/S0016756822000991>

Received: 16 June 2022
Revised: 18 August 2022
Accepted: 31 August 2022

Keywords:

planktonic foraminifera; middle Cenomanian Event 1 (MCE 1); palaeoceanography; carbon and oxygen stable isotopes; England

Author for correspondence:

Maria Rose Petrizzo,
Email: mrose.petrizzo@unimi.it

Planktonic foraminifera document palaeoceanographic changes across the middle Cenomanian carbon-isotope excursion MCE 1: new evidence from the UK chalk

Maria Rose Petrizzo¹  and Andy S Gale^{2,3}

¹Dipartimento di Scienze della Terra “A. Desio”, Università degli Studi di Milano, via Mangiagalli 34, Milan 20133, Italy; ²School of the Environment, Geography and Geological Sciences, University of Portsmouth, Burnaby Building, Burnaby Road, Portsmouth PO13 QL, UK and ³Department of Earth Science, The Natural History Museum, Cromwell Road, London SW7 5BD, UK

Abstract

Planktonic foraminifera were studied at Lydden Spout, near Folkestone (southeast England, UK), the reference section of the middle Cenomanian Event 1 (MCE 1) characterized by a prominent double-peak $\delta^{13}\text{C}$ excursion of 1 ‰ identified in different ocean basins and considered a global event. Biostratigraphic and quantitative analysis of planktonic foraminifera are correlated to the $\delta^{13}\text{C}$ perturbation, to the positive $\delta^{18}\text{O}$ shifts identified within MCE 1 and to the occurrence of Boreal macrofossils (the bivalves *Chlamys arlesiensis* and *Oxytoma seminudum*, and the belemnite *Praectinocamax primus*). Variations in abundance and species richness of planktonic foraminifera and the inferred palaeoecological preferences of taxa permit the identification of distinct palaeoenvironmental settings across MCE 1. The stratigraphic interval corresponding to MCE 1 is characterized by the absence of oligotrophic rotaliporids, and by the evolutionary appearance of meso-eutrophic dicarinellids and of *Muricohedbergella portsdownensis*, a cold-water species that occurs at the same level as the Boreal macrofossils. These observations indicate a palaeoceanographic scenario characterized by reduced stratification of surface waters and absence/disruption of the thermocline in a dominantly eutrophic regime during MCE 1. Evidence provided by planktonic foraminifera, Boreal macrofossils and $\delta^{18}\text{O}$ records documented for the late Cenomanian Plenus Cold Event (PCE) at Eastbourne (UK) reveal similarities that confirm the periodic inflow of cold Boreal seawater originating in the Norwegian Sea as previously postulated to explain the occurrence of Boreal fauna in the Anglo-Paris Basin. The southerly extension of this water mass may be related to the reorganization of circulation driven by the long eccentricity cycle.

1. Introduction

This study presents a detailed analysis of the middle Cenomanian planktonic foraminifera from the Lydden Spout section near Folkestone (Kent, UK) (Fig. 1). This section is particularly important because it records the middle Cenomanian Event 1 (MCE 1), a carbon isotope excursion first described by Paul *et al.* (1994) in northwest European sections from the Anglo-Paris Basin and Cleveland Basin, that is characterized by a prominent double-peak $\delta^{13}\text{C}_{\text{carb}}$ positive excursion of up to 1 ‰ named MCE 1 by Mitchell *et al.* (1996) in a study of the $\delta^{13}\text{C}$ record at Folkestone, Speeton in the Cleveland Basin (North Yorkshire, UK), and Wünstorf in the Lower Saxony Basin. In these sections, Mitchell *et al.* (1996) described the lower isotopic peak of the bipartite excursion as MCE 1a and the upper one as MCE 1b, and observed that the early portion above MCE 1b has a relatively flat $\delta^{13}\text{C}$ signature followed by increasing $\delta^{13}\text{C}$ values that at Speeton and Folkestone are interrupted by a small negative $\delta^{13}\text{C}$ excursion that was named MCE 2.

The MCE 1 is a globally recognized carbon cycle perturbation that has been identified in the US Western Interior Basin (Gale *et al.* 2008; Joo & Sageman, 2014; Eldrett *et al.* 2015; Ma *et al.* 2022), Atlantic Ocean (Ando *et al.* 2009; Friedrich *et al.* 2009; Hardas *et al.* 2012), northern Europe (Wilmsen, 2003, 2007; Voigt *et al.* 2004; Erbacher *et al.* 2020), Italy (Erbacher *et al.* 1996; Stoll & Schrag, 2000; Coccioni & Galeotti, 2003; Gambacorta *et al.* 2015), France (Giraud *et al.* 2013; Reboulet *et al.* 2013), Spain (Rodríguez-Lazaro *et al.* 1998), north Africa (Kuhnt *et al.* 2009; Gertsch *et al.* 2010; Beil *et al.* 2018) and Tibet (Li *et al.* 2006). Changes in benthic and planktonic foraminifera, radiolaria, calcareous nannofossils and nektonic assemblages characterize the MCE 1 (e.g. Paul *et al.* 1994; Erbacher *et al.* 1996; Mitchell & Carr, 1998; Rodríguez-Lazaro *et al.* 1998; Coccioni & Galeotti, 2003; Wilmsen *et al.* 2005, 2007; Friedrich *et al.* 2009; Hardas *et al.* 2012), but the interpretations of these changes are

© The Author(s), 2022. Published by Cambridge University Press. This is an Open Access article, distributed under the terms of the Creative Commons Attribution licence (<http://creativecommons.org/licenses/by/4.0/>), which permits unrestricted re-use, distribution and reproduction, provided the original article is properly cited.



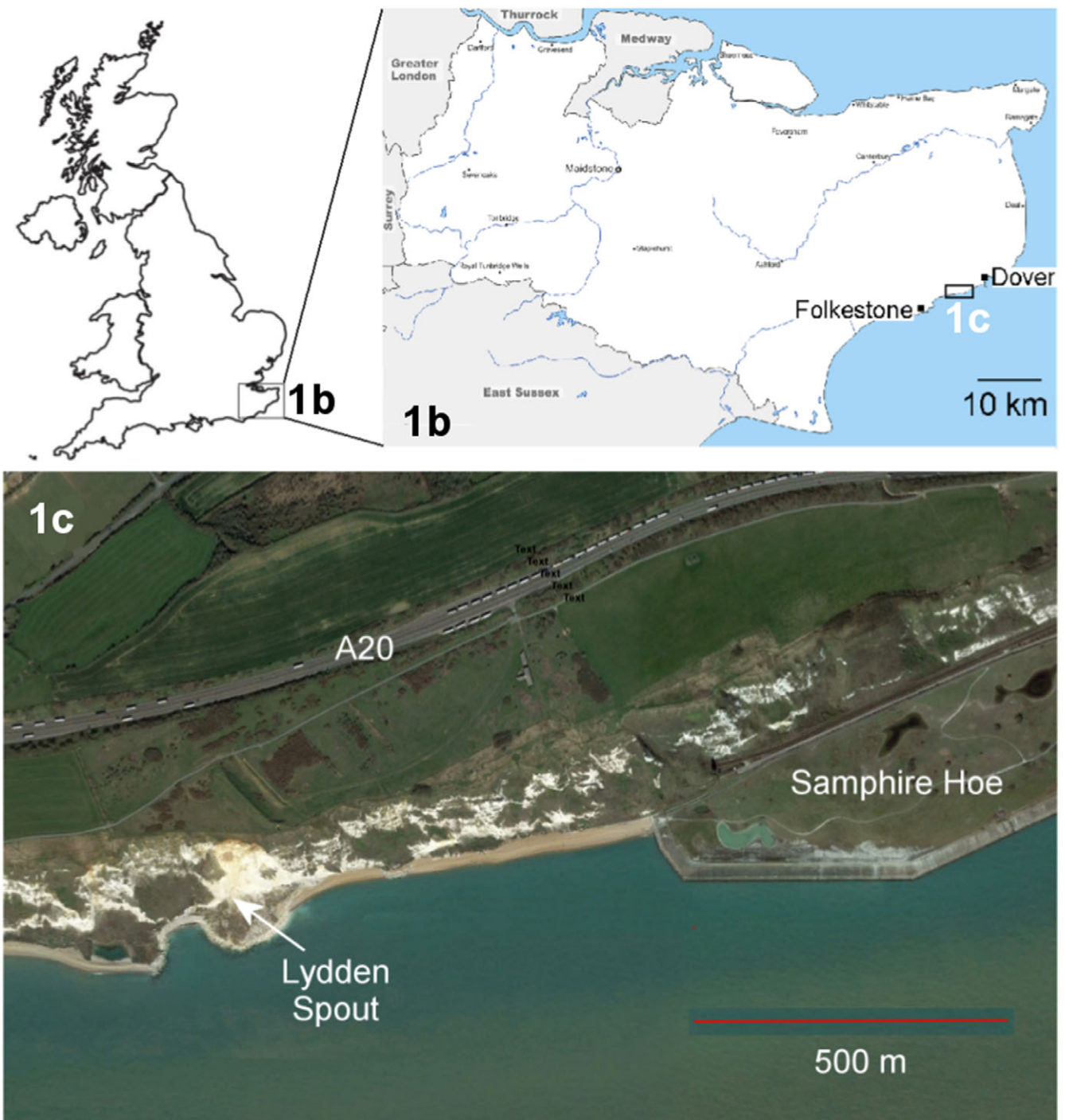


Fig. 1. (Colour online) (a) Map of the British Isles. (b) Location of the section between Dover and Folkestone in Kent. (c) Google Earth image of region west of Samphire Hoe to show location of Lydden Spout.

contradictory. For instance, the benthic foraminiferal assemblages suggest that the MCE 1 was associated with dysaerobia of lower-intermediate water masses (Basque Basin, Spain: Rodriguez-Lazaro *et al.* 1998), stratification of the water column (Anglo-Paris Basin: Mitchell & Carr, 1998; tropical Atlantic Ocean: Friedrich *et al.* 2009; Hardas *et al.* 2012) or decreased ventilation on the sea floor (Umbria-Marche Basin, Italy: Coccioni & Galeotti, 2003). The MCE 1 was interpreted as an event of increased marine primary productivity (Umbria-Marche Basin: Erbacher &

Thurow, 1997; Stoll & Schrag, 2001; Coccioni & Galeotti, 2003; northern Germany: Wilmsen, 2003), but in the tropical Atlantic Ocean, calcareous nannofossils indicate increased stratification of the water column that resulted in more oligotrophic conditions of the upper photic zone (Hardas *et al.* 2012). In the Basque Basin, planktonic foraminiferal assemblages do not change across the MCE 1 (Rodriguez-Lazaro *et al.* 1998), whereas they vary in composition and size throughout the excursion in the Anglo-Paris Basin (Paul *et al.* 1994). Radiolarian assemblages of the western

Tethys and the North Atlantic show an extinction of 26 % of all species, and the loss of deep habitats was interpreted as being related to the expansion of the oxygen minimum zone during sea-level rise (Erbacher *et al.* 1996).

The MCE 1 was proposed as a precursor to the late Cenomanian – early Turonian Oceanic Anoxic Event 2 (OAE 2, e.g. Jenkyns, 2010), although of lower amplitude (e.g. Coccioni & Galeotti, 2003; Friedrich *et al.* 2009; Zheng *et al.* 2016) and currently much less well understood than OAE 2. The location of the carbon-burial sink responsible for the MCE 1 positive carbon-isotope excursion is poorly known, but Gale (1995, fig. 11) noted the presence of laminated, organic-rich sediments at one level in the Vocontian Basin (southeast France). Laminated black shales corresponding to the $\delta^{13}\text{C}$ positive excursion also occur in the tropical Atlantic Ocean (Demerara Rise, total organic content values from 5 to 18 %, Friedrich *et al.* 2009).

The relationships between MCE 1 and OAE 2 are poorly constrained, although similarities and differences are observed. In western Europe, boreal belemnites (*Praectinocamax primus*) and bivalves (*Chlamys arlesiensis* and *Oxytoma seminudum*) spread southwards during the MCE 1, indicating two cooling pulses (e.g. Paul *et al.* 1994; Gale & Christensen, 1996; Wilmsen, 2003). Similarly, a southward incursion of boreal assemblages containing *Praectinocamax plenus* characterizes cooling episodes known as the Plenus Cold Event (PCE; Gale & Christensen, 1996; Jarvis *et al.* 2011; Jenkyns *et al.* 2017; Gale *et al.* 2019a; O'Connor *et al.* 2019) that interrupted the supergreenhouse conditions during part of the Cenomanian–Turonian positive $\delta^{13}\text{C}$ excursion that identifies the OAE 2.

The MCE 1 and OAE 2 differ in the amplitude and shape of the $\delta^{13}\text{C}$ excursion and in the rates of organic carbon burial. The size of the MCE 1 excursion is smaller than the 2–3 ‰ positive excursion recorded during OAE 2 and is of shorter duration (Jarvis *et al.* 2006; Joo & Sageman, 2014; Eldrett *et al.* 2015; Gambacorta *et al.* 2015). Astronomical age models from the US Western Interior Seaway indicate a duration of c. 0.21 Ma for the MCE 1 compared to the estimation of OAE 2 that varies between 0.52 and 0.92 Ma (Sageman *et al.* 2006; Eldrett *et al.* 2015; Batenburg *et al.* 2016).

The carbon isotope record during the onset of the MCE 1 and OAE 2 suggests comparable triggering mechanisms and climate–carbon cycle feedbacks during the two events, although there is no undeniable evidence for a similar initiation mechanism. Volcanic activity and emplacement of Large Igneous Provinces (LIPs: Caribbean, High Arctic, Madagascar and Ontong-Java) were suggested to be responsible for the initiation of OAE 2. For instance, evidence of volcanism based on the osmium-isotope record suggests that a major pulse of volcanism and associated sea-floor hydrothermal weathering began prior to the onset of the carbon isotope excursion at the base of OAE 2 (e.g. Turgeon & Creaser, 2008; Du Vivier *et al.* 2014, 2015; Jenkyns *et al.* 2017). Neodymium-isotope positive excursion during OAE 2 in the European epicontinental sea (Zheng *et al.* 2013) and in the tropical Atlantic Ocean (MacLeod *et al.* 2008; Martin *et al.* 2012) were interpreted to reflect transport of radiogenic neodymium released from LIP volcanism under anoxic conditions. By contrast, no neodymium-isotope increase was observed across the MCE 1 (Jiménez Berrocoso *et al.* 2010; Zheng *et al.* 2016), although its record supports reorganization of ocean circulation during the MCE 1 and OAE 2 and high productivity in surface waters, with nutrients probably deriving from deep waters and/or LIPs sources (Zheng *et al.* 2016). According to Scaife *et al.* (2017), sedimentary

mercury concentration data from the US Western Interior Seaway and North Atlantic Ocean are consistent with an initial magmatic pulse at the time of the MCE 1 followed by a second greater pulse at the onset of OAE 2, possibly related to the emplacement of LIPs in the Pacific Ocean and/or the High Arctic.

Cenomanian times (100.5–93.9 Ma) register one of the best-documented episodes of eustatic rise in sea-level in Earth history and the beginning of the Late Cretaceous Thermal Maximum, driving the global expansion of epicontinental seas and the onset of widespread pelagic and hemipelagic carbonate deposition (e.g. Giorgioni *et al.* 2015). It was also a time when the evolutionary diversification of planktonic foraminifera took place at a fast rate. After the major turnover across the Aptian–Albian boundary interval (Kennedy *et al.* 2000; Leckie *et al.* 2002; Huber & Leckie, 2011; Petrizzo *et al.* 2012, 2013; Kennedy *et al.* 2014), the progressive appearance of new lineages is observed throughout the Albian and Cenomanian.

A marked phase of high evolutionary rates is registered in the Cenomanian within the polyphyletic *Rotalipora* group (*Rotalipora* Brotzen, 1942; *Thalmanninella* Sigal, 1948; *Pseudothamanninella* Wonders, 1978; *Parathalmanninella* Lipson-Benitah, 2008), that includes trochospiral taxa with sutural or umbilical supplementary aperture and a peripheral keel (Wonders, 1980; González-Donoso *et al.* 2007). Rotaliporids are the major component of the assemblages until the end of the Cenomanian when the last representative (*Rotalipora cushmani*) disappears. The morphological plasticity and species variation within the *Rotalipora* lineages (e.g. Robaszynski *et al.* 1994; Petrizzo & Huber, 2006; González-Donoso *et al.* 2007; Lipson-Benitah, 2008) has influenced the planktonic foraminiferal biozonation (e.g. Ando *et al.* 2010; Petrizzo *et al.* 2015; Falzoni *et al.* 2018; Petrizzo & Gilardoni, 2020). Specifically, the classic Tethyan biozonations made by Robaszynski & Caron (1995) and Premoli Silva & Sliter (1995), that were incorporated in the Geological Time Scales (Gradstein *et al.* 2004, 2012; Ogg *et al.* 2016; Gale *et al.* 2020 in Gradstein *et al.* 2020), have recently been revised by Petrizzo and Gilardoni (2020) who introduced the *Thalmanninella greenhornensis* Zone. This is defined as the stratigraphic interval between the lowest occurrence (LO) of *T. greenhornensis* and the LO of *R. cushmani*, to overcome the difficulty in identifying the *Thalmanninella reicheli* Zone of previous authors because of the rarity and absence of the species in many western and eastern Tethyan localities and in the US Western Interior Basin record. The appearance of *T. greenhornensis* is demonstrated to be an easy identifiable bioevent as the species is characterized by a wider geographic distribution and is often reported to appear in the same stratigraphic level as *T. reicheli* when the latter species is present (see discussion in Petrizzo & Gilardoni, 2020). Moreover, the middle to late Cenomanian planktonic foraminiferal record is also characterized by the evolutionary appearance of the unkeeled trochospiral and heavily muricate *Whiteinella* and of the double-keeled genera *Dicarinella* and *Marginotruncana* (Premoli Silva & Sliter, 1995; Fraass *et al.* 2015; Falzoni *et al.* 2018; Falzoni & Petrizzo, 2020; Petrizzo & Gilardoni, 2020).

In this study, the planktonic foraminifera stratigraphic distribution, abundance, species richness and population dynamics are coupled with the inferred palaeoecological preferences of taxa to interpret the palaeoceanographic changes and the trophic features of the surface waters across the MCE 1 positive $\delta^{13}\text{C}$ excursion, which is also characterized by a series of positive $\delta^{18}\text{O}$ shifts indicating episodes of remarkable cooling.

2. Folkestone section: background and methods

2.a. Location and stratigraphy

The sea-cliff at Lydden Spout, 500 m west of Samphire Hoe, on the coast between Folkestone and Dover, Kent (Fig. 1), provides 25 m of accessible exposure of lower and middle Cenomanian chalks of the Westbury and Zigzag Chalk Formations (Fig. 2). The chalks are rhythmically bedded on a scale of several decimetres, darker marly levels alternating with paler chalky beds, interpreted as precession cycles driven by dilution from the input of clay (Gale *et al.* 1999). The stratigraphy and ammonite zonation of the succession between Dover and Folkestone was described by Kennedy (1969). The detailed stratigraphy of the middle Cenomanian succession at Lydden Spout was illustrated by Gale (1989), who provided a detailed log and identified a succession of distinctive beds which could be correlated across the Anglo-Paris Basin (Gale, 1990, 1995). These papers also demonstrated the presence of macrofossil taxa with Boreal affinities at this level, previously recorded from the upper part of the late Cenomanian Plenus Marl Member (Jefferies, 1962, 1963). These include two species of bivalve, *Chlamys arlesiensis* and *Oxytoma seminudum*, and a nektonic belemnite, *Praectinocamax*. In the middle Cenomanian, Boreal species are concentrated in a lower *C. arlesiensis* Bed and a higher *P. primus* Bed (Fig. 2; Gale, 1995: the Cast Bed of Gale, 1989).

2.b. The stable carbon-isotope and oxygen-isotope record

A positive carbon isotope excursion containing two peaks was identified in the lower part of the middle Cenomanian of the Lydden Spout succession by Paul *et al.* (1994) and was correlated with detailed records of macrofossils and foraminifera. This carbon isotope excursion was subsequently named MCE 1 by Mitchell *et al.* (1996; see also Jarvis *et al.* 2006) who described the lower peak of the bipartite excursion as MCE 1a and the upper peak as MCE 1b. The MCE 1a begins in the *Cunningtoniceras inerme* ammonite Zone (Jarvis *et al.* 2001, 2006), and is associated with a lowstand systems tract (Gale, 1995; Gale & Kennedy, 2021); the MCE 1b falls in the lowermost part of the ammonite *Acanthoceras rhotomagense* Zone (Jarvis *et al.* 2001, 2006) and is associated with a transgressive systems tract (Gale, 1995; Mitchell *et al.* 1996).

The carbon isotope record at Folkestone in the studied stratigraphic interval records the MCE 1 excursion (Fig. 2) similar to that reported by Paul *et al.* (1994) and Zheng *et al.* (2016). In this study, bulk-chalk $\delta^{13}\text{C}$ was measured every ~5 cm and registered peak values of ~2.5 ‰ in the *C. arlesiensis* Bed at 31.7 m which are followed by a trough of ~2.2 ‰ and by a subsequent $\delta^{13}\text{C}$ rise to ~2.5 ‰ toward the top of the *P. primus* Bed before decreasing again at ~35.2 m (Fig. 2). The stratigraphic position of the double-peak $\delta^{13}\text{C}$ positive excursion is in agreement with that reported by Paul *et al.* (1994), although $\delta^{13}\text{C}$ values are slightly different between the two studies. Here we define the MCE 1 event as the positive carbon excursion extending from the rise in values at the base of the *C. arlesiensis* Bed (31.5 m), to the fall in values at 36 m (Fig. 2).

The $\delta^{18}\text{O}$ bulk carbonate record at Folkestone documents cyclic fluctuations within MCE 1 related to individual couplets with heavier values in marls and lighter values in chalks (Fig. 2; Paul *et al.* 1994; Voigt *et al.* 2004) that indicate a primary temperature change in sea-surface waters (Ditchfield & Marshall, 1989). The interval from 31.5 to 34 m registers the heaviest values, with a positive peak of 1.68 ‰ in the *C. arlesiensis* Bed at 31.75 m followed by subsequent positive peaks of 1.95 ‰ at 32.55 m, 2.0 ‰ at 33.3 m, and 2.07 ‰ at 33.85 m; the latter peak is registered in the *P. primus*

Bed (Fig. 2; Supplementary Material Table S1). The observed $\delta^{18}\text{O}$ positive peaks in the *C. arlesiensis* Bed and in the *P. primus* Bed were also previously documented by measurements on brachiopod shells collected from Lydden Spout (Voigt *et al.* 2004; Gale & Kennedy, 2021).

2.c. Sequence stratigraphy

There are marked changes in sea-level during the MCE 1 in the Anglo-Paris Basin, interpreted from sequence-stratigraphical analysis (Robaszynski *et al.* 1998) as representing the boundary between their Cenomanian sequences 3 and 4 (see summary in Gale & Kennedy, 2021). The sequence boundary at the top of sequence Ce3 has been identified within the upper *Mantelliceras dixonii* Zone, and over the London Platform, to the north, this surface erodes down into older Cenomanian chalks. Subsequent sea-level rise, commencing at the time of deposition of the *C. arlesiensis* Bed and Cast Bed, resulted in onlap of the condensed Totternhoe Stone (*Acanthoceras rhotomagense* Zone) over lower Cenomanian chalks across the Transitional Province of southern England (Gale & Kennedy, 2021). The Lydden Spout succession is uncondensed and was deposited in shallow waters (<200 m) in a pelagic epicontinental environment at the junction of the Boreal Sea, Tethys and proto-North Atlantic. The Ce3–Ce4 sequence boundary has been identified very widely, from the US Western Interior (Gale *et al.* 2008), Texas (Eldrett *et al.* 2015), Germany (Wilmsen, 2003, 2007), north Africa (Kuhnt *et al.* 2009), Ukraine and Kazakhstan (Gale *et al.* 1999) and southeast India (Gale *et al.* 2019b). The events involved sea-level fall and subsequent rise of c. 30 m over a relatively short timespan (200 kyr) based on observation of precession cycles (Gale, 1995).

A sustained cooling phase that may even have resulted in ephemeral glaciations in Antarctica was also suggested for the MCE 1 based on a bulk carbonate $\delta^{18}\text{O}$ increase in combination with sequence-stratigraphic evidence for a high-amplitude sea-level fall from the Contessa Quarry (Gubbio, Umbria–Marche Basin, Italy) and the New Jersey Coastal Plain (Stoll & Schrag, 2000; Miller *et al.* 2003, 2005). Significant cooling pulses during the MCE 1 were determined from brachiopod shells from the mid-latitude shelf of Europe, including Folkestone, by Voigt *et al.* (2004) that, to the contrary, related it to major reorganization of ocean circulation in the North Atlantic that probably favoured increased oceanic ventilation and upwelling of nutrient-rich waters. Subsequently, the middle Cenomanian glaciation hypothesis was challenged by isotope records of glassy planktonic and benthic foraminifera that did not indicate a measurable ice volume signal in $\delta^{18}\text{O}$ records across the MCE 1 (Moriya *et al.* 2007; Ando *et al.* 2009).

2.d. Planktonic foraminifera

The Lydden Spout section was sampled for planktonic foraminiferal analyses using a sampling resolution of c. 50 cm from 26.70 to 42.75 m (Fig. 2). A total of 32 samples were processed following the standard procedure using hydrogen peroxide to obtain washed residues for micropaleontological analyses. Biostratigraphic and quantitative analyses were carried out for all the washed residues of the >125 μm size-fraction. In addition, the 125–38 μm size-fraction was scanned for marker species. Abundance counts of planktonic vs benthic foraminifera were made by microsplitting samples to obtain aliquots of equal volume for all samples, from which the foraminifera were counted (Supplementary Material Table S2).

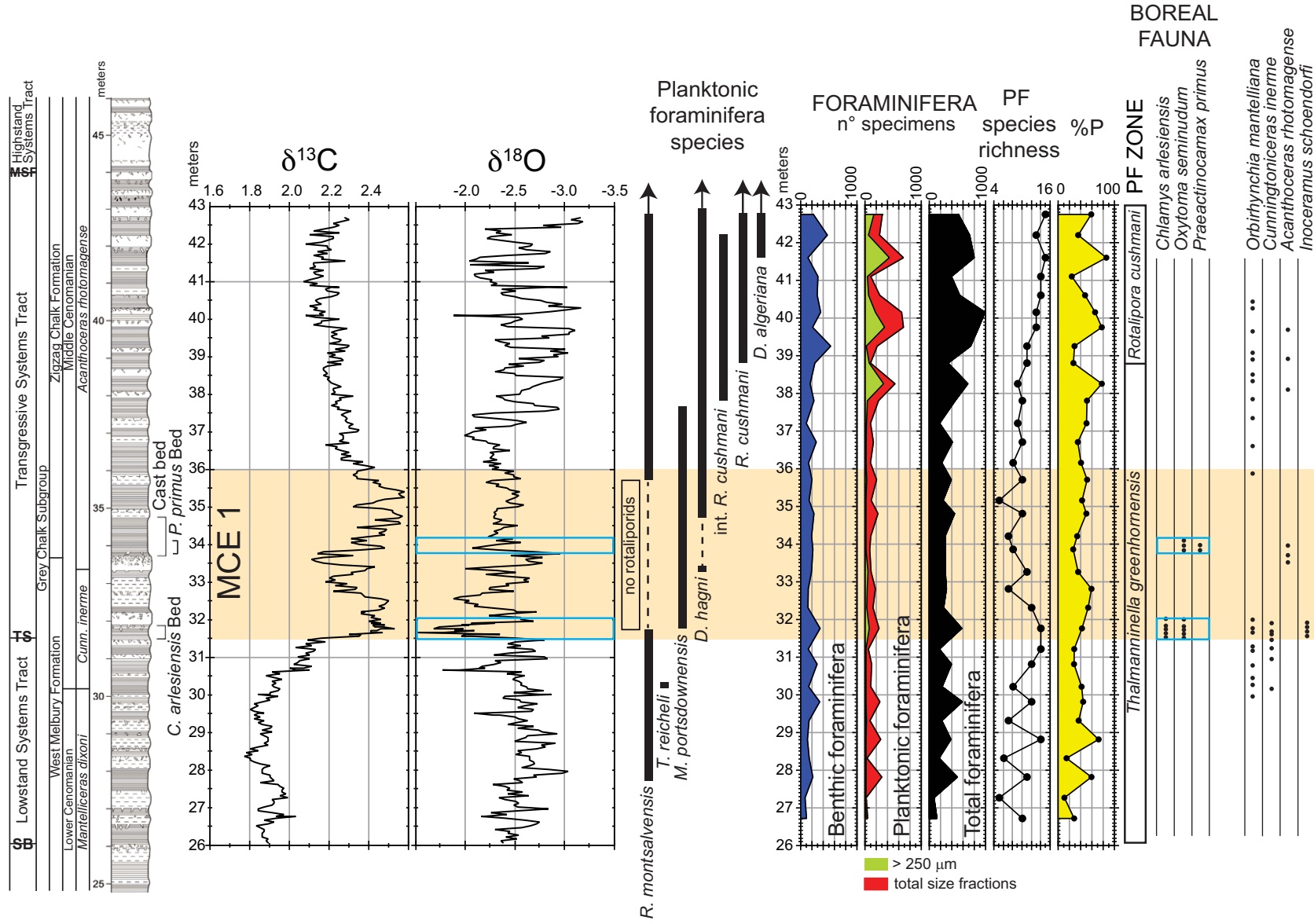


Fig. 2. (Colour online) Succession of Cenomanian chalk at Lydden Spout, Folkestone, showing sequence-stratigraphic interpretation (Gale & Kennedy, 2021), lithostratigraphy (Gale, 1989) and ammonite biostratigraphy (Wright *et al.* 2017). The carbon-isotope and oxygen-isotope curves are based on 5 cm spaced samples, analysed at Cambridge University in 1997. The data show the double carbon-isotope positive excursion of the MCE 1. The *Chlamys arlesiensis* Bed, *Praeactinocamax primus* Bed and Cast Bed are according to Gale (1995). Foraminiferal abundances, planktonic foraminiferal species distribution and species richness and per cent planktonic foraminifera (% P) according to this study. Planktonic foraminifera zonation after Petrizzo & Gilardoni (2020). To the right are records of important macrofaunal elements, including benthic macrofossils with Boreal affinities, ammonites and an inoceramid bivalve (Gale & Kennedy, 2021). Light orange band = middle Cenomanian Event 1 (MCE 1); light blue rectangles = δ¹⁸O positive peaks and occurrence of Boreal fauna; PF = planktonic foraminifera.

Planktonic foraminiferal genera and species were identified according to holotypes and paratypes illustrated on the pforams@mikrotax portal (Huber *et al.* 2016, online taxonomic dictionary updated by the Mesozoic Planktonic Foraminifera Working Group, <http://www.mikrotax.org/pforams/index.html>) and in the Ellis and Messina Catalogues (Micropaleontology Press, <http://www.micropress.org/em/>). In addition, several publications were used to ameliorate the species identification (i.e. Caron & Spezzaferri, 2006; Ando & Huber, 2007; González-Donoso *et al.* 2007; Desmares *et al.* 2008; Georgescu, 2009; Petrizzo *et al.* 2015; Huber *et al.* 2022). Biozonation follows Petrizzo and Gilardoni (2020).

3. Composition and distribution of the planktonic foraminiferal assemblage

The foraminiferal population in the size-fraction >125 µm is composed of planktonic and benthic foraminifera that are almost equally abundant, although the proportion of planktonic foraminifera as a percentage of the total foraminiferal assemblage (% P) shows values between 30 and 50 % in one-third of the samples and only in eight samples are planktonic foraminifera less than 30 % (% P: Fig. 2; Supplementary Material Table S2). However, planktonic foraminifera are always rare in the >250 µm size-fractions and they are totally absent at the base of the section from 26.70 to 29.30 m and within the upper part of the MCE 1 interval from 34.20 to 35.70 m (Fig. 2). An increase in total abundance of both benthic and planktonic foraminifera is observed from above 38 m, and the latter group exceeds 50 % of the foraminiferal assemblage in almost all samples (Fig. 2; Supplementary Material Table S2).

The planktonic foraminiferal assemblage shows poor to moderate preservation that improves toward the top of the studied section. Diversity ranges from 6 species near the base to 15 species at the top except for a minimum value of 5 species recorded in the upper part of the MCE 1 interval above the *P. primus* Bed (Fig. 2; Supplementary Material Table S2).

The most common and abundant species that consistently occur throughout the section are *Muricohedbergella delrioensis*, *Pseudoclavihedbergella simplicissima*, *Praeglobotruncana stephani*, *Praeglobotruncana delrioensis*, *Praeglobotruncana cf. compressa* and *Whiteinella brittonensis* (Table 1). Keeled rotaliporids show a scattered occurrence, are limited to the lower and the upper part of the studied section and are absent in the stratigraphic interval from 32.80 to 35.15 m within the MCE 1 interval (from the peak values of ~2.5 ‰ in the *C. arlesiensis* Bed to the second peak value of ~2.5 ‰ above the *P. primus* Bed). *Thalmaninella reicheli* and *Thalmaninella micheli* are only observed at 30.20 and 30.80 m, respectively. One specimen of *Thalmaninella deckeei* was present at 31.75 m (Table 1). The lowest occurrence of *Rotalipora cushmani* is recorded at 38.80 m and is preceded by forms that show intermediate features between *Rotalipora montsalvensis* and *R. cushmani*. *Muricohedbergella portdownensis* have a restricted stratigraphic range from 25 cm above the base of MCE 1 at 31.75 m to 1.80 m above the termination of the MCE 1 at 37.80 m. The evolutionary appearance of the double-keeled *Dicarinella* is marked by the subsequent first occurrence of *D. hagni* within the MCE 1 at 33.25 m and of *D. takayanagii* at 38.80 m and of *D. algeriana* at 41.60 m. *Helvetoglobotruncana praealpetica* is first observed at 38.80 m (Table 1).

4. Planktonic foraminifera biozonation

According to the composition of the assemblages and the position of the marker events, the stratigraphic interval from the base of the studied section at 26.70 m to 38.80 m is assigned to the *Thalmaninella greenhornensis* Zone, whereas the interval above is assigned to the *Rotalipora cushmani* Zone (Fig. 2). No specimens of *T. greenhornensis* were found in the assemblages; however, the occurrence of *Whiteinella aprica* from the base of the studied section (Table 1) demonstrates that the stratigraphic interval corresponds to the upper part of the *T. greenhornensis* zone following the biozonation by Petrizzo and Gilardoni (2020). This assignment is supported by the presence of a rare specimen of *T. reicheli* at 30.20 m, of *R. montsalvensis* that occurs from 27.80 m upwards, of *Thalmaninella gandolfii* first observed at 28.80, and of *T. deckeei* identified at 31.75 m (Fig. 2; Table 1).

5. Comparison with previous studies of the planktonic foraminiferal assemblages at Folkestone

Comparison of the data acquired in this study with those obtained in previous studies on the same stratigraphic sequence (Paul *et al.* 1994; Mitchell & Carr, 1998; Moghadam & Paul, 2000) highlights some differences. In the present study, the appearance of *R. cushmani* is recorded at 38.80 m whereas it was first observed by Paul *et al.* (1994) above this level at c. 40.5 m. The difference is minor and is probably related to the different sampling resolution (1 m in Paul *et al.* 1994 compared to 50 cm in this study), to the preservation of the specimens and to the rarity of the first representatives of *R. cushmani*. In fact, *R. cushmani* evolved from *R. montsalvensis* (González-Donoso *et al.* 2007; Petrizzo & Gilardoni, 2020) and occurs together with common specimens that are morphologically transitional with its ancestor, making the identification of the first *R. cushmani* sometimes difficult to detect (Ando *et al.* 2015; Erbacher *et al.* 2020).

A discrepancy is also observed in the stratigraphic range of *T. reicheli* which was found in only one sample below the MCE 1 level at 30.20 m in this study. Moghadam and Paul (2000) recorded *T. reicheli* at c. 30.5 m. Paul *et al.* (1994) reported *T. reicheli* from two samples below these levels at c. 28–29 m. By contrast, only Mitchell and Carr (1998) observed specimens related to *T. reicheli* (identified as *Rotalipora ex gr. reicheli*) discontinuously occurring from the base of the section to within the MCE 1 level at c. 34 m. These differences in the identification of *T. reicheli* are not surprising considering the known discontinuous occurrences and rarity of this species in many Tethyan localities (northern Israel: Lipson-Benitah *et al.* 1997; southern Spain, central Tunisia and northern Italy: Wonders, 1980; Poland: Peryt, 1983; Dubicka & Machalski, 2017) and in the western North Atlantic Ocean (Blake Nose: Bellier *et al.* 2000), and its absence in the US Western Interior Seaway (Pessagno, 1969; Eicher & Worstell, 1970; Denne *et al.* 2014; Eldrett *et al.* 2015) and northern California (Douglas, 1969), that limit its reliability for intra- and inter-basin correlation. *Favusella washitensis*, observed by Paul *et al.* (1994) and Mitchell and Carr (1998) within the MCE 1 level at c. 34–35 m, has not been observed in this study.

A significant increase in the proportion of planktonic foraminifera was first recognized by Carter and Hart (1977) in the middle Cenomanian of southern England and northern France and was suggested to record a significant break in the succession; the

Table 1. Distribution of planktonic foraminiferal species in the Lydden Spout section

Samples	metres	<i>Muricohedbergella crassa</i>	<i>Muricohedbergella delrioensis</i>	<i>Laevella bentonensis</i>	<i>Praeglobotruncana cf. compressa</i>	<i>Thalmaninella brotzeni</i>	<i>Whiteinella baltica</i>	<i>Pseudoclavihedbergella simplicissima</i>	<i>Rotalipora praemontsalvensis</i>	<i>Whiteinella aprica</i>	<i>Whiteinella brittonensis</i>	<i>Planoheterohelix moremani</i>	<i>Rotalipora montsalvensis</i>	<i>Muricohedbergella planispira</i>	<i>Praeglobotruncana stephani</i>	<i>Planohedbergella ultramirca</i>	<i>Pseudoclavihedbergella amabilis</i>	<i>Whiteinella paradubia</i>	<i>Praeglobotruncana delrioensis</i>	<i>Thalmaninella gandolfii</i>	<i>Thalmaninella globotruncanoides</i>	<i>Thalmaninella reicheli</i>	<i>Thalmaninella micheli</i>	<i>Whiteinella aumalensis</i>	<i>Praeglobotruncana oraviensis</i>	<i>Praeglobotruncana gibba</i>	<i>Thalmaninella deeckeii</i>	<i>Muricohedbergella cf. portsdowensis</i>	<i>Dicarinella hagni</i>	intermediate <i>Rotalipora cushmani</i>	<i>Dicarinella takayanagii</i>	<i>Helvetoglobotruncana praehelvetica</i>	<i>Rotalipora cushmani</i>	<i>Dicarinella algeriana</i>
A+11	42.75		X	X			X			X		X	X	X		X									X		X	X	X		X	X		
A+10.5	42.20		X	X	X			X		X		X		X		X							X				X	X	X		X			
A+10	41.60	X	X		X				X	X		X	X	X				X		X							X	X	X					X
A+9.5	41.10		X		X			X		X		X	X	X		X	X			X								X	X				X	
A+9	40.60	X	X		X			X	X	X		X	X	X		X							X				X		X				X	
A+8.5	40.15	X	X		X			X		X		X	X	X		X		X					X				X	X			X	X		
A+8	39.75		X		X			X	X	X		X	X	X		X	X						X		X			X						
A+7.5	39.25		X		X				X		X		X	X		X							X				X	X			X	X		
A+7	38.80		X		X			X		X		X	X	X				X							X				X	X	X			
A+6.5	38.25		X	X	X			X				X	X	X				X							X		X							
A+6	37.80		X			X	X			X				X				X							X		X	?	X					
A+5.5	37.20			X	X			X					X	X	X			X									X	X						
A+5	36.70		X		X		X	X				X	X	X	X		X	X										X						
A+4.5	36.15	X	X		X									X				X					X				X	X						
A+4	35.70	X	X		X								X	X				X					X		X		X							
A+3.5	35.15		X		X			X						X													X	X						
A+3	34.80	X	X		X			X		?	X						X	X					X				X							
A+2.5	34.20		X	X			X										X									X		X						
A+2	33.85		X				X	X			X			X			X	X											X					
A+1.5	33.25		X	X	X			X						X			X	X							X		X	X						
A+1	32.80		X				X	X						X										X					?					
A+0.5	32.30	X	X		X		X	X						X			X	X								X		X						
A0	31.75		X		X			X		X				X			X	X					X	X	X	X	X	X						
A-0.5	31.20	X	X		X		X	X						X			X	X							X	X								

(Continued)

Table 1. (Continued)

Samples	metres	<i>Muricohedbergella crassa</i>	<i>Muricohedbergella delrioensis</i>	<i>Laeviella bentonensis</i>	<i>Praeglobotruncana cf. compressa</i>	<i>Thalmaninella brotzeni</i>	<i>Whiteinella baltica</i>	<i>Pseudoclavihedbergella simplicissima</i>	<i>Rotalipora praemontsalvensis</i>	<i>Whiteinella aprica</i>	<i>Whiteinella brittonensis</i>	<i>Planoheterohelix moremani</i>	<i>Rotalipora montsalvensis</i>	<i>Muricohedbergella planispira</i>	<i>Praeglobotruncana stephani</i>	<i>Planohedbergella ultramicra</i>	<i>Pseudoclavihedbergella amabilis</i>	<i>Whiteinella paradubia</i>	<i>Praeglobotruncana delrioensis</i>	<i>Thalmaninella gandolfii</i>	<i>Thalmaninella globotruncanoides</i>	<i>Thalmaninella reicheli</i>	<i>Thalmaninella micheli</i>	<i>Whiteinella aumalensis</i>	<i>Praeglobotruncana oraviensis</i>	<i>Praeglobotruncana gibba</i>	<i>Thalmaninella deeckeii</i>	<i>Muricohedbergella cf. portsdownensis</i>	<i>Dicarinella hagni</i>	intermediate <i>Rotalipora cushmani</i>	<i>Dicarinella takayanagii</i>	<i>Helvetoglobotruncana prae-helvetica</i>	<i>Rotalipora cushmani</i>	<i>Dicarinella algeriana</i>			
A-1	30.80	X				X	X		?	X		X		X	X	X	X					X			X												
A-1.5	30.20	X												X		X		X			X		X	X													
A-2	29.80		X	X			X	X		X	X		X		X		X	X	X	X																	
A-2.5	29.30	X	X				X	X								X		X																			
A-3	28.80		X	X		X	X	X		X	X		X	X	X	X	X	X		X																	
A-3.5	28.30		X		X		X	X					X				X																				
A-4	27.80	X	X	X			X	X	X	X	X	X	X		X																						
A-4.5	27.25	X	X				X	X								X																					
A-5	26.70	X	X	X	X	X	X		X	X																											

so-called 'mid-Cenomanian non-sequence'. Subsequently, the abrupt increase in abundance of planktonic foraminifera proved to be a useful marker horizon, named the P/B break (a level at which the proportion of planktonics increases from c. 5 % to as much as 50 %) by Paul *et al.* (1994), and also identified in other stratigraphic sections of the Anglo-Paris Basin (Mitchell *et al.* 1996; Moghadam & Paul, 2000), coinciding with the first occurrence of *R. cushmani* or falling close to the base of its stratigraphic range. In the Cenomanian of the Anglo-Paris Basin, values of % P in excess of 40 % have not been recorded below the appearance level of *R. cushmani* (Hart *et al.* 1989; Paul *et al.* 1994) and only Mitchell and Carr (1998) reported % P higher than 40 % in the *C. arlesiensis* Bed at c. 32 m in the Folkestone section. By contrast, our data reveal that the abundance of planktonic foraminifera exceeds 50 % at only a few levels throughout the stratigraphic section studied (Fig. 2). The P/B break is placed at c. 40.5 m at Folkestone by Paul *et al.* (1994) and Moghadam and Paul (2000); we record a systematic increase of planktonic foraminifera with values higher than 50 % from above the termination of the MCE 1 interval at 37.80 to the top of the section, although in this interval some samples show lower % P values (23 to 34 %; Fig. 2; Supplementary Material Table S2). Therefore, we continue to use the term P/B break as employed in previous publications as we observe a cyclic alternation in abundance of the foraminiferal assemblages in the upper part of the section.

Paul *et al.* (1994) documented a decrease in size of rotaliporids and muricohedbergellids (= *Hedbergella* in Paul *et al.* 1994) in the lower part of the MCE 1 interval from 31 to 34 m that has not been observed in the current study. The reasons for this discrepancy are difficult to explain in the absence of detailed information on how the decrease in size was measured by Paul *et al.* (1994) who analysed samples with 1 m resolution, examined the >250 μm size-fraction and only scanned the smaller size-fractions for smaller species. In the present study, samples were collected at 50 cm intervals and the size-fractions >125 μm were studied. Interestingly, we observed planktonic foraminifera larger than 250 μm only in the interval where Paul *et al.* (1994) observed the decrease in size (31 to 34 m); by contrast, the increase in size near the top of the section from 40 to 42 m (at the P/B break) shown by Paul *et al.* (1994) correlates with our data documenting an increase in abundance of planktonic foraminifera in the >250 μm size-fraction (Fig. 2).

6. Palaeoceanographic inferences

The planktonic foraminiferal assemblage in the middle Cenomanian at Folkestone is composed of common muricohedbergellids and praeglobotruncanids followed in abundance by whiteinellids, rotaliporids and dicarinellids. The palaeoenvironmental setting can be determined by considering the palaeoecological preferences of Cenomanian planktonic foraminiferal taxa which are mainly based on their stable isotope ($\delta^{18}\text{O}$ and $\delta^{13}\text{C}$) composition, and on their biogeographic distributions across latitudes, with additional information provided by their abundances. Studies focused in near-coastal, hemipelagic and pelagic settings indicate that planktonic foraminifera may have tolerated variations in salinity levels and are capable of completing their life cycles in both shallow- and deeper-water environments (e.g. Leckie, 1987; Hart, 1999; Huber *et al.* 1999; Premoli Silva & Sliter, 1999; Bornemann & Norris, 2007; Petrizzo *et al.* 2008, 2020; Ando *et al.* 2010).

According to the literature (see reviews in Petrizzo *et al.* 2020 and Falzoni & Petrizzo, 2022), *Rotalipora* and *Thalmaninella*

inhabited cold/deep layers of the water column close to the thermocline, although with some differences observed among species and through time. Rotaliporids found in pelagic settings of the Tethyan Realm have been interpreted as oligotrophic, and thus required a relatively thick and stratified upper water column to complete their life cycle. Muricohedbergellids are adapted to relatively cold/deep layers of the water column in open ocean settings at low latitudes (Norris & Wilson, 1998; Wilson *et al.* 2002; Petrizzo *et al.* 2008; Ando *et al.* 2010), but they may have inhabited shallower layers at the higher latitudes of the Southern Hemisphere, probably because sea-surface waters were cooler (Falzoni *et al.* 2016; Petrizzo *et al.* 2020, 2021, 2022a,b). Moreover, muricohedbergellids are commonly found in low-salinity coastal environments to normal-salinity open-ocean settings, indicating they had an opportunist meso-eutrophic life strategy (e.g. Leckie, 1987, 1998; Hart, 1999; Premoli Silva & Sliter, 1999). *Praeglobotruncana* species have been interpreted as intermediate- or winter mixed-layer dwellers (Petrizzo *et al.* 2008, 2020; Falzoni *et al.* 2016), and adapted to cool and poorly stratified surface waters (Ando *et al.* 2010). *Dicarinella* were adapted to cold waters and lived close to the permanent thermocline in different localities at low to middle latitudes (Huber *et al.* 1999; Wendler *et al.* 2013; Falzoni *et al.* 2016; Petrizzo *et al.* 2020). Data from the Southern Hemisphere indicate a shallower habitat at higher latitudes (Petrizzo *et al.* 2020, 2021, 2022a,b). Therefore, water depth, ocean circulation patterns (e.g. currents) and boundaries between different water masses (Schiebel & Hemleben, 2017) are the main factors controlling the presence or absence of taxa in ecological niches. Other ecological factors are the thickness of the mixed layer, the position and stability of the thermocline, trophic conditions, and salinity (e.g. Hart, 1999; Abramovich *et al.* 2003; Ando *et al.* 2009, 2010; Falzoni *et al.* 2013, 2016; Petrizzo *et al.* 2017; and discussions therein).

Our knowledge of the palaeoecological preferences of planktonic foraminifera coupled with their abundance and distribution is consistent with a palaeoceanographic scenario at Folkestone that implies changes in circulation patterns. Specifically, in the MCE 1 interval the absence of the thermocline-dwelling oligotrophic rotaliporids is balanced by the appearance of the intermediate-depth and cold-water adapted dicarinellids. Moreover, the assemblage is characterized by the relatively high abundance of the eutrophic-mesotrophic *Praeglobotruncana* and *Muricohedbergella*. Interestingly, *M. portsdownensis*, a species also documented as occurring in the middle Cenomanian record of the North German Basin at Wünstorf (Erbacher *et al.* 2020), shows a stratigraphic distribution limited to the carbon isotope excursion identifying the MCE 1 at Folkestone. The species first appears in the *C. arlesiensis* Bed at the same level of the occurrence of Boreal macrofossils species and coincident with a positive $\delta^{18}\text{O}$ shift of 1 ‰ and disappears slightly after the termination of the MCE 1 at the level (37.80 m) that records the increase in % P and the appearance of the intermediate forms between *R. montsalvensis* and *R. cushmani* (Fig. 2). According to the observed record we infer that *M. portsdownensis* had a meso-eutrophic life strategy, proliferated in cold water and is probably a Boreal species. However, further studies are needed to confirm the stratigraphic and geographical distribution of this species which has rarely been mentioned in the literature, and, as discussed in the Taxonomic remarks section further below, additional studies are required to investigate its possible synonymy with *Muricohedbergella kyphoma*, a species coinciding with the coldest episode (Falzoni & Petrizzo, 2022) of the late Cenomanian Plenus Cold Event (PCE).

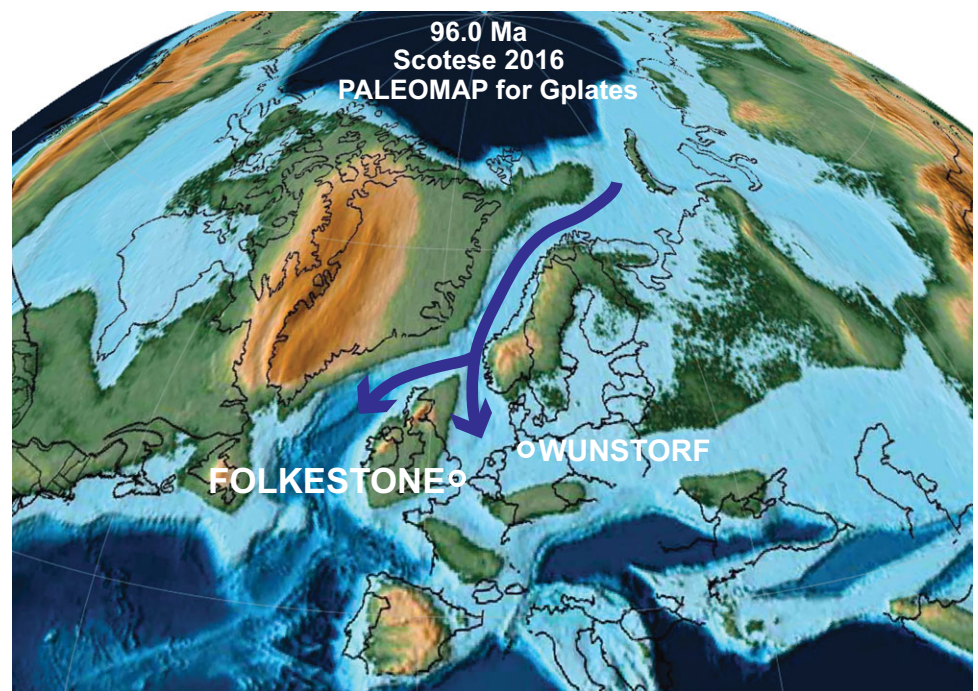


Fig. 3. (Colour online) Palaeogeographic reconstruction (Scotese, 2016) for the middle Cenomanian (96 Ma) with location of Folkestone (UK) and Wünstorf (Germany). The blue arrow shows the inferred inflow into the Anglo-Paris seaway and North German Basin of cold Boreal waters.

7. Remarks on the cooling pulses within the MCE 1 and comparison with the Plenian Cold Event (PCE)

At Lydden Spout, and in other sections in the Anglo-Paris Basin, the occurrence of Boreal benthic macrofossils (*C. arlesiensis*, *O. seminudum* and *P. primus*) is recorded within the MCE 1 $\delta^{13}\text{C}$ excursion (Paul *et al.* 1994; Gale, 1995) and coincides with a positive excursion in $\delta^{18}\text{O}$ (Voigt *et al.* 2004; Gale & Kennedy, 2021) and isotopically light neodymium values (Zheng *et al.* 2016). The shelf–sea cooling pulses observed within the MCE 1 at the *C. arlesiensis* Bed and *P. primus* Bed by Voigt *et al.* (2004) were interpreted as coinciding with transgressive phases during a major third-order sea-level lowstand and reflecting a major reorganization of the North Atlantic circulation.

Our new oxygen-isotope data (bulk chalk) through MCE 1 at Lydden Spout (Fig. 2; Supplementary Material Table S1) show a heavy shift of *c.* 1 ‰ in the *C. arlesiensis* Bed. This level is precisely coincident with the base of the MCE 1 carbon-isotope excursion, the occurrence of Boreal macrofossils, the disappearance of rotaliporids and the appearance of *M. portdownensis*. This change translates into a cooling of *c.* 4 °C (temperature equation of Anderson & Arthur, 1983), probably in sea-surface waters as the values are derived from calcareous nannofossils in the bulk sediment. Brachiopod shells through the *C. arlesiensis* Bed (Gale & Kennedy, 2021, fig. 6) also show a 1 ‰ heavy shift in $\delta^{18}\text{O}$, but to values which are consistently 1 ‰ heavier than those from the bulk sediment record. These data thus provide evidence of a significant temperature gradient from the surface to the sea floor (*c.* 4 °C) in the middle Cenomanian Chalk Sea. The fluctuating values of $\delta^{18}\text{O}$ coincide precisely with the boundaries of chalk:marl couplets, and heavier values are consistently present in the marls, lighter values in chalks. The absolute heavy values of $\delta^{18}\text{O}$ decrease progressively in the three couplets succeeding the *C. arlesiensis* Bed (Fig. 2). The couplets have been identified as precession cycles (Gale *et al.* 1999) and it can therefore be argued that orbital forcing was a primary control on the fluctuating temperature values.

The cold-water planktonic foraminiferal assemblages occurring in the MCE 1 interval indicate the presence of poorly thermally stratified water masses characterized by a reduced/collapsed thermocline that disrupted the ecological niches of the oligotrophic rotaliporids which, thus, are totally absent in the MCE 1 interval at Folkestone (Fig. 2). Keel planktonic foraminifera are also absent across the MCE 1 interval identified in the Boreal North German Basin at Wünstorf, and their absence was controlled by sea-level changes in an epicontinental sea where environmental conditions were unsuitable for keel planktonic foraminiferal species (Erbacher *et al.* 2020).

Together, these observations indicate that the enhanced influence of Boreal seawater in the European epicontinental sea resulted in a sensitive response of ocean circulation to climate fluctuations and support the hypothesis of the inflow into the Anglo-Paris seaway of cold Boreal waters originating in the Norwegian Sea (Fig. 3). A similar interpretation was proposed to explain the planktonic foraminiferal assemblage changes and the occurrence of the Boreal macrofauna *C. arlesiensis*, *O. seminudum* and *P. plenius* in the PCE interval at Eastbourne (UK) (O'Connor *et al.* 2019; Falzoni & Petrizzo, 2022).

Comparison between the planktonic foraminiferal assemblages during the cooling episodes within the MCE 1 and those occurring at the PCE reveals a similar composition, with dominance of taxa more adapted to cooler and relatively poorly stratified water masses (*Muricohedbergella*, *Praeglobotruncana*, *Dicarinella*). Additional evidence for a Boreal origin of these assemblages is provided by the occurrence of common *M. portdownensis* at Folkestone and *M. kyphoma* at Eastbourne (Falzoni & Petrizzo, 2022). Regardless of the taxonomic assignments of these species (as explained in the Taxonomic remarks section further below), they are only observed in the levels containing Boreal macrofossils and are therefore interpreted as mesotrophic–eutrophic species that did not require a thermally stratified water column. The absence of oligotrophic rotaliporids in the MCE 1 interval at Folkestone and the extinction in the PCE interval of *R. cushmani*

(the last representative of the rotaliporid group) are probably related to the ingress of cold Boreal waters that temporally disrupted the stratified oligotrophic water column. Therefore, the equatorward expansion of the Boreal macrofossils and the dominance of cold-water and meso-eutrophic planktonic foraminifera observed at the MCE 1 and PCE may reflect cyclic latitudinal shifts of the proto-Arctic Front of *c.* 10–20° that forced a major reorganization of the surface and deep ocean circulation patterns in the middle and late Cenomanian (Zheng *et al.* 2016; Falzoni & Petrizzo, 2022). Using an orbitally tuned dataset, Batenburg *et al.* (2016) suggested that the MCE 1 and OAE 2 carbon isotope events were driven by the long eccentricity cycle (mode at 2.4 Ma) with positive excursions coincident with minima. In parallel, the southerly extensions of cold Boreal water during the MCE 1 and the PCE may also have been caused by long eccentricity-driven reorganization of ocean circulation.

8. Conclusions

Planktonic foraminifera at Folkestone were studied across the MCE 1 positive $\delta^{13}\text{C}$ excursion and are correlated with the occurrence of Boreal macrofossils and of heavy $\delta^{18}\text{O}$ excursions in bulk carbonate values, indicating a cooling of *c.* 4 °C. In general, planktonic foraminifera stratigraphically below the MCE 1 level indicate a pelagic epicontinental environment characterized by a stratified water column with a well-defined mixed layer and a thin thermocline, as confirmed by the occurrence of both surface- and deep-water dwelling taxa. This palaeoenvironmental setting is interrupted at the onset of the $\delta^{13}\text{C}$ excursion of the MCE 1 as revealed by changes in the composition of the planktonic foraminiferal assemblage and in the stratigraphic distribution of species. The double-keeled *Dicarinella* first evolved within the MCE 1, indicating the availability of favourable ecological niches in a thick mixed layer. By contrast, the total absence of the single-keeled rotaliporids within the MCE 1 interval is interpreted to reflect a substantial disruption of water mass stratification and of the ecological niches occupied by the thermocline-dwelling oligotrophic rotaliporids. Cooling phases within the MCE 1 are also confirmed by the occurrence of the Boreal macrofossils *C. arlesiensis*, *O. seminudum* and *P. primus*, the occurrences of which identify the *C. arlesiensis* Bed and *P. primus* Bed. Remarkable is the appearance of the species *M. portdownensis* at the base of the MCE 1 interval at the same level of the occurrence of Boreal benthic macrofossils (*C. arlesiensis* Bed). This observation suggests that *M. portdownensis* was a surface and cold-water dweller and it is probably a useful middle Cenomanian marker species that permits identification of the MCE 1 interval. After the termination of the perturbation associated with the MCE 1, planktonic foraminifera increase in abundance and species richness as testified by the occurrence of keeled and deep-water species, indicating the return of a stratified water column with a mixed layer and well-defined thermocline.

Overall, the planktonic foraminiferal assemblages recorded in the MCE 1 interval reflect conditions of eutrophy associated with cold surface waters. In addition, the occurrence of Boreal benthic fauna associated with heavy oxygen isotope excursions provides evidence of cooling episodes which might coincide with transgressive mixing over the epicontinental Anglo-Paris Basin. These falls in temperature possibly resulted from the southerly extension of cold Boreal low-salinity and poorly stratified water masses which originated in the Norwegian Sea, as previously postulated to explain the occurrence of Boreal macrofossils within the positive $\delta^{13}\text{C}$ excursion that identifies MCE 1. Finally, similarities in the composition of benthic

macrofossils and planktonic foraminiferal assemblages, and in the heavy oxygen isotope excursions which occurred during the MCE 1 and the PCE, suggest that two latitudinal shifts of the proto-Arctic Front of *c.* 10–20° took place in these intervals. The changes may be related to orbital configurations driven by long eccentricity maxima (cf. Batenburg *et al.* 2016).

9. Taxonomic remarks

Foraminifera genera and species with authors and years identified in the studied sediments (Table 1) are listed in alphabetical order and comments are included for some species so as to clarify the taxonomic concepts followed in this study. Remarks on significant morphological and evolutionary features are provided when necessary. Selected species are illustrated in Figs. 4–7.

Genus *Dicarinella* Porthault, 1970.

Type species: *Globotruncana indica* Jacob & Sastry, 1950, p. 267, fig. 2A–C.

Dicarinella algeriana (Caron, 1966), pp. 74–5, pl. 16, fig. 8 (lower Turonian, Sidi Aïssa, Algeria).

Dicarinella hagni (Scheibnerova, 1962), pp. 225–6, fig. 6 (middle Turonian, Horné Srnie, west Carpathians, Czechoslovakia).

Dicarinella takayanagii Hasegawa, 1999, p. 187, fig. 8, fig. 3A–C (uppermost Cenomanian, Takinosawa Formation, Hokkaido, Japan).

Genus *Helvetoglobotruncana* Reiss, 1957.

Type species: *Globotruncana helvetica* Bolli, 1945, pp. 226, 227, pl. 9, figs 6–8 (middle Turonian, 'Knollen-Schichten', eastern Switzerland).

Helvetoglobotruncana praehelvetica (Trujillo, 1960) p. 340, pl. 49, fig. 6 (early Turonian, California).

Genus *Laeviella* Huber, Petrizzo & Falzoni, 2022.

Type species: *Anomalina bentonensis* Morrow, 1934, p. 201, pl. 30, figs 4a–b (Cenomanian, Hartland Member of Greenhorn Limestone of Kansas).

Laeviella bentonensis (Morrow, 1934), p. 201, pl. 30, figs 4a–b (Cenomanian, Hartland member of Greenhorn Limestone of Kansas).

Remarks. Previously included in *Globigerinelloides*, see taxonomic revision in Huber *et al.* (2022).

Genus *Muricohedbergella* Huber and Leckie (2011).

Type species: *Globigerina cretacea* var. *delrioensis* Carsey (1926, pp. 43–4).

Muricohedbergella crassa (Bolli, 1959), p. 265, figs 1–2 (Upper Cretaceous, Naparima Hill formation, Trinidad).

Muricohedbergella delrioensis (Carsey, 1926), pp. 43–4 (lower Cenomanian, Del Rio Clay, Grayson Formation, Austin, TX).

Muricohedbergella planispira (Tappan, 1940), p. 12, pl. 19, fig. 12 (Cenomanian, Grayson Formation, Denton County, TX).

Muricohedbergella portdownensis (Williams-Mitchell, 1948), p. 96, pl. 8, fig. 4 (Cenomanian, Portdown No. 1 well, Hampshire, England).

Remarks. It is an overlooked species rarely reported in the literature (Loeblich & Tappan, 1961; Pessagno, 1967; Douglas & Rankin, 1969; Hermes, 1969; Eicher & Worstell, 1970). The species was discussed by Carter and Hart (1977) who inspected the holotype and regarded it as falling into the species variability of *Hedbergella delrioensis*. Moreover, Carter and Hart (1977) included in *Whiteinella brittonensis* the specimens previously identified as *portdownensis* by reason of having a high trochospire. The examination of the image of the holotype reproduced in

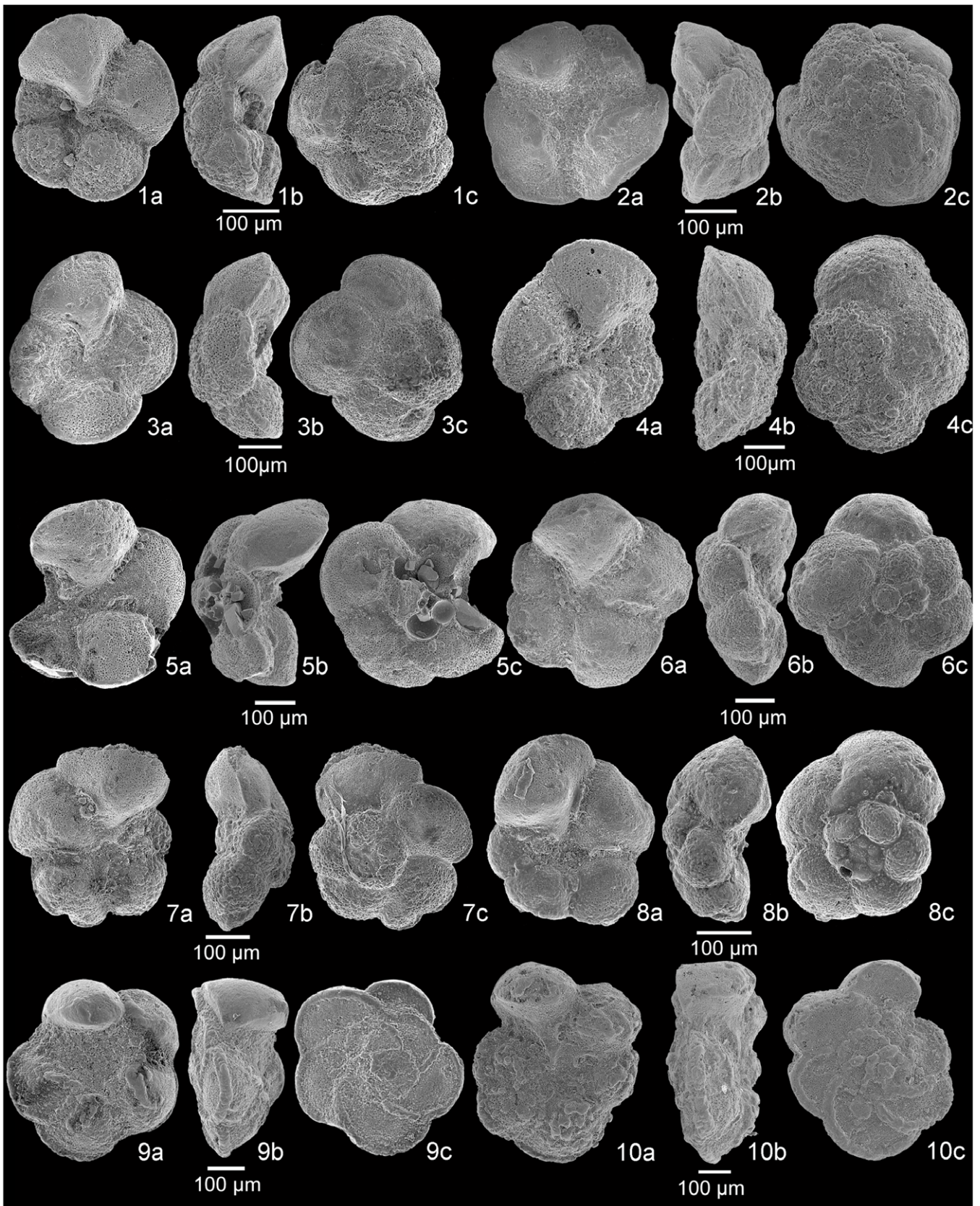


Fig. 4. Scanning electron microscope (SEM) images of planktonic foraminifera. 1a–c, *Rotalipora cushmani*, sample A+11. 2a–c, *Rotalipora cushmani*, sample A+10.5. 3a–c, *Rotalipora cushmani*, sample A+9. 4a–c, *Rotalipora cushmani*, sample A+7. 5a–c, intermediate form between *Rotalipora montsalvensis* and *Rotalipora cushmani*, sample A+6. 6a–c, *Rotalipora montsalvensis*, sample A+4. 7a–c, *Rotalipora montsalvensis*, sample A 0. 8a–c, *Rotalipora praemontsalvensis*, sample A--4. 9a–c, *Thalmanninella micheli*, sample A-1. 10a–c, *Thalmanninella reicheli*, sample A-1.5. a, umbilical view; b, side view; c, spiral view.

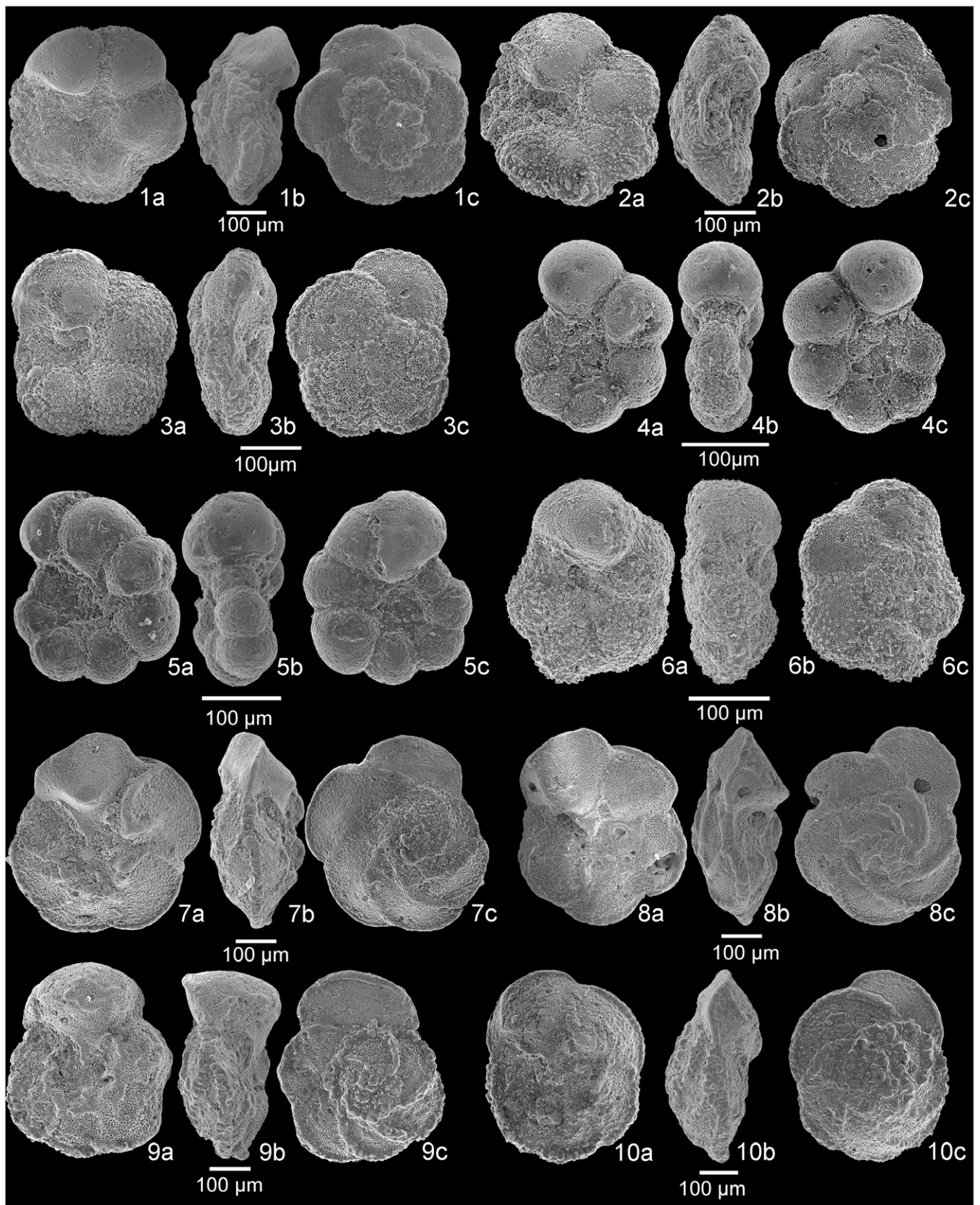


Fig. 5. SEM images of planktonic foraminifera. 1a–c, *Dicarinella hagni*, sample A+10.5. 2a–c, *Dicarinella algeriana*, sample A+11. 3a–c, *Dicarinella takayanagii*, sample A+10. 4a–c, *Laeviella bentonensis*, sample A+11. 5a–c, *Laeviella bentonensis*, sample A+1.5. 6a–c, *Helvetoglobotruncana praehelvetica*, sample A+7. 7a–c, *Thalmaninella globotruncanoides*, sample A+10. 8a–c, *Thalmaninella globotruncanoides*, sample A+9.5. 9a–c, *Thalmaninella gandolfii*, sample A–2. 10a–c, *Thalmaninella brotzeni*, sample A+6. a, umbilical view; b, side view; c, spiral view.

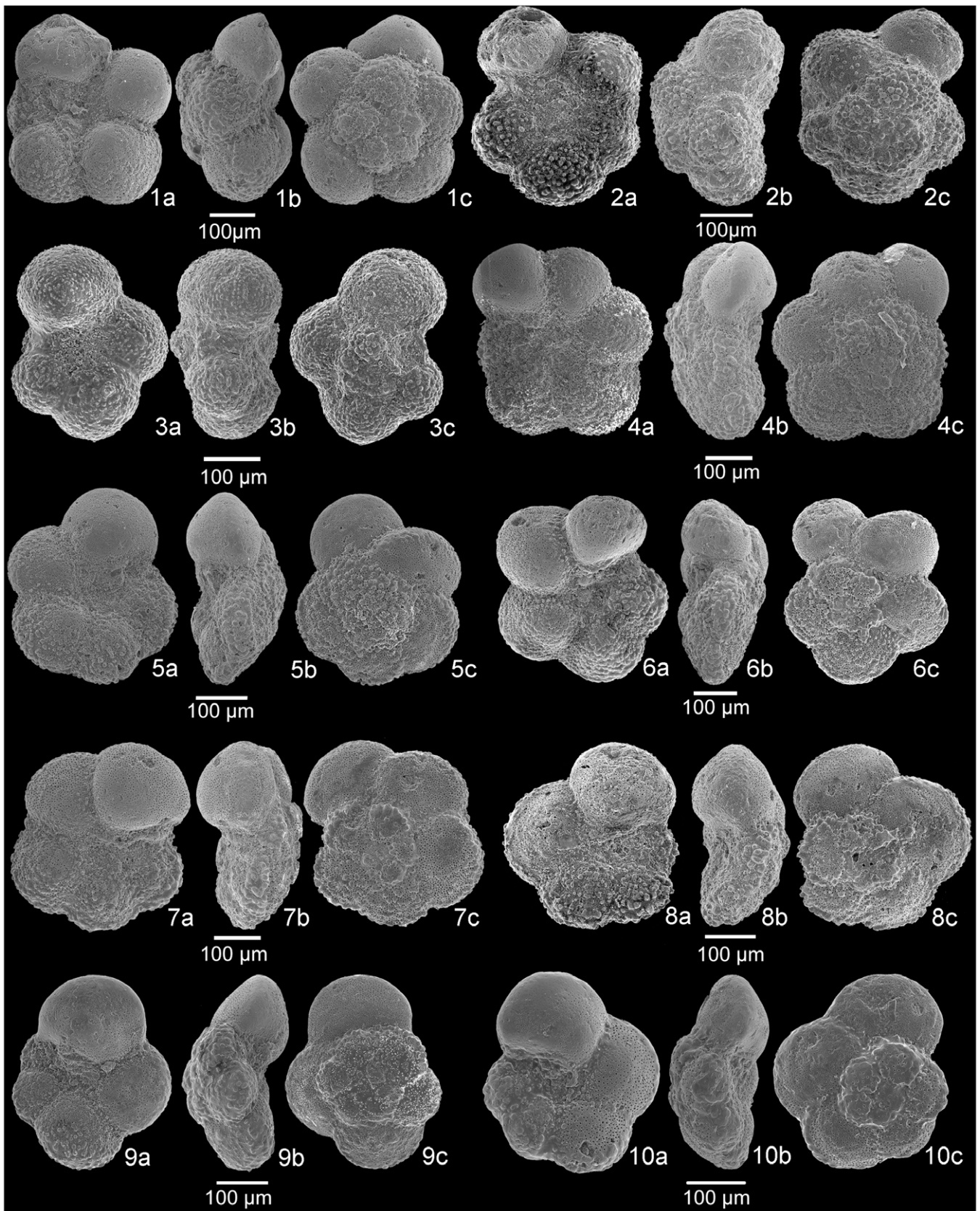


Fig. 6. SEM images of planktonic foraminifera. 1a–c, *Whiteinella brittonensis*, sample A+7.5. 2a–c, *Whiteinella paradubia*, sample A 0. 3a–c, *Whiteinella baltica*, sample A–5. 4a–c, *Whiteinella aumalensis*, sample A+8.5. 5a–c, *Praeglobotruncana stephani*, sample A+10.5. 6a–c, *Praeglobotruncana oraviensis*, sample A 0. 7a–c, *Praeglobotruncana delrioensis*, sample A–1.5. 8a–c, *Praeglobotruncana delrioensis*, sample A+6. 9a–c, *Praeglobotruncana cf. compressa*, sample A+5.5. 10a–c, *Praeglobotruncana cf. compressa*, sample A+0.5. a, umbilical view; b, side view; c, spiral view.

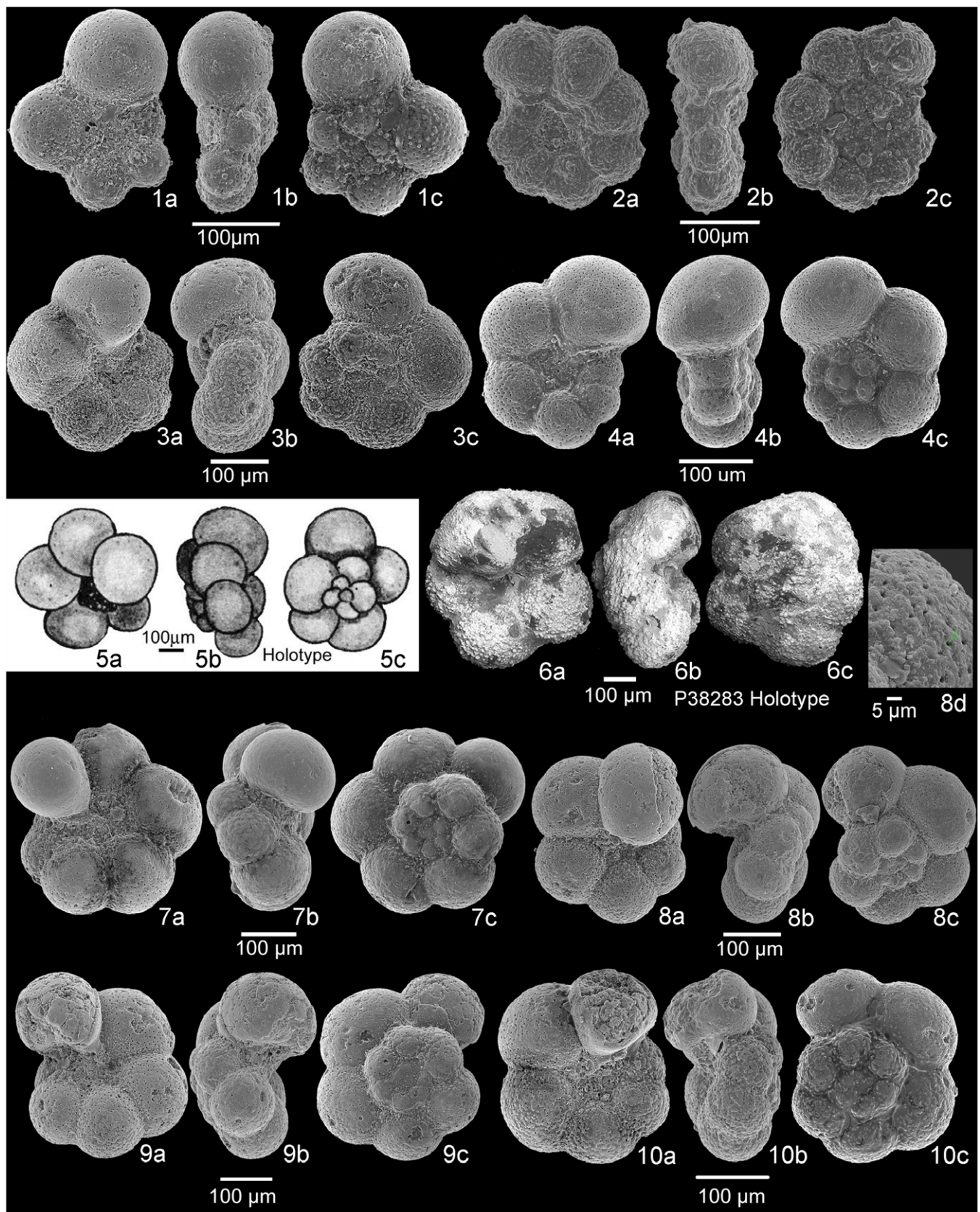


Fig. 7. SEM images of planktonic foraminifera. 1a–c, *Pseudoclavhedbergella simplicissima*, sample A–4. 2a–c, *Muricohedbergella planispira*, sample A+5. 3a–c, *Muricohedbergella delrioensis*, sample A+11. 4a–c, *Muricohedbergella crassa*, sample A–5. 5a–c, *Globigerina portdownensis*, illustrated holotype P 38283 (repository Natural History British Museum) from Williams-Mitchell (1948). 6a–c, *Muricohedbergella portdownensis*, holotype P 38283 (image from www.mikrotax.org). 7a–c, *Muricohedbergella portdownensis*, sample A+5. 8a–d, *Muricohedbergella portdownensis*, sample A+5.5. 9a–c, *Muricohedbergella portdownensis*, sample A+4. 10a–c, *Muricohedbergella portdownensis*, sample A+3. a, umbilical view; b, side view; c, spiral view; d, detail.

Fig. 7(5a–c) confirms that *portsdownensis* is morphologically very similar to *W. brittonensis*, but in our opinion it differs by having a low trochospire and a slightly muricate wall texture instead of heavy pustules and by having the last two chambers of the final whorl smooth. Recently, *M. portsdownensis* was identified by Erbacher *et al.* (2020) in the North German Basin occurring in the stratigraphic interval across the MCE.

Muricohedbergella portsdownensis is very similar to *Muricohedbergella kyphoma*, a species described from Japan (Hasegawa, 1999) as occurring discontinuously from below the first appearance of *Rotalipora cushmani* to above the extinction of *R. cushmani*. The species has been recognized within the Plenus Cold Event (PCE) at Eastbourne and Clot Chevalier (Gale *et al.* 2019a) by Falzoni & Petrizzo (2020, 2022) in the interval recording the extinction of *R. cushmani* and the occurrence of the Boreal macrofossils (*C. arlesiensis* and *P. plenus*), and thus interpreted as a marker species indicative of the coolest episodes of the PCE.

Muricohedbergella portsdownensis and *M. kyphoma* are here regarded as separate species although the possibility that they are morphotypes of the same species cannot be excluded since they show a similar muricate and pustulose wall texture and only differ by the sutures on the ultimate chambers of the spiral side that are curved in *M. kyphoma* and straight in *M. portsdownensis*. However, for the time being, we separate the two species until detailed stratophenetic studies of the planktonic foraminiferal assemblages are performed in stratigraphic sections containing a continuous record from the interval below the MCE 1 to the interval above the PCE in order to investigate the timing and the mode in the evolution and distribution of the two species.

Genus *Planohedbergella* Boudagher-Fadel, Banner, Whittaker & McCarthy, 1997, in BouDagher-Fadel *et al.* (1997), emended Huber *et al.* (2022).

Type species: *Planomalina ehrenbergi* Barr, 1962 [= *Planomalina yaucoensis* Pessagno 1960].

Planohedbergella ultramicra (Subbotina, 1949), p. 33, pl. 2, figs 17–18 (Cenomanian, Kapustnaya Gorge, southern slope of Caucasus, Russia).

Remarks. Previously included in *Globigerinelloides*, see taxonomic revision in Huber *et al.* (2022).

Genus *Planoheterohelix* Georgescu and Huber (2009).

Type species: *Planoheterohelix postmoremani* Georgescu and Huber (2009), p. 346, pl. 5, figs 1–11.

Planoheterohelix moremani (Cushman, 1938), p. 10, pl. 2, figs 1, 2 (Cenomanian, Eagle Ford Shale, Texas, USA).

Genus *Praeglobotruncana* Bermudez (1952).

Type species: *Globorotalia delrioensis* Plummer (1931), p. 199, pl. 13, fig. 2.

Praeglobotruncana compressa Hasegawa (1999), p. 181, fig. 5, 5A–C (upper Cenomanian, Takinosawa Formation, Hokkaido, Japan).

Remarks. The specimens identified in this study as *P. cf. compressa* closely resemble the holotype of *P. compressa* and only differ by having a slightly high trochospire and a biconvex lateral profile.

Praeglobotruncana delrioensis (Plummer, 1931), p. 199, pl. 13, fig. 2 (Lower Cretaceous, Del Rio Formation, on right bank of Shoal Creek, Austin, Travis Country, TX).

Praeglobotruncana stephani (Gandolfi, 1942), p. 130, pl. 3, fig. 4 (Cenomanian, Gorge of the Breggia River, near Chiasso, southeastern Switzerland).

Praeglobotruncana gibba Klaus (1960), pp. 209, 304–5, pl. 16–17, fig. 6a–c (Cenomanian, Gorge of the Breggia River, near Chiasso, southeastern Switzerland).

Praeglobotruncana oraviensis Scheibnerova (1960), p. 87, tf. 4A–C (lower Turonian, Czechoslovakia).

Genus *Pseudoclavihedbergella* Georgescu (2009).

Type species: *Hedbergella amabilis* Loeblich and Tappan (1961), p. 274, pl. 3, figs 1–10.

Pseudoclavihedbergella amabilis Loeblich and Tappan (1961), p. 274, pl. 3, figs 1–10 (Cenomanian, Britton Clay, Eagle Ford Group, Texas).

Pseudoclavihedbergella simplicissima (Magné & Sigal, 1954), p. 487, pl. 14, fig. 11 (lower Cenomanian, Rhazouane, Tunisia).

Genus *Rotalipora* Brotzen (1942).

Type species: *Rotalipora turonica* Brotzen (1942), p. 32, text-fig. 11–4, = *Globorotalia cushmani* Morrow (1934), p. 199, pl. 31, fig. 4.

Rotalipora cushmani (Morrow, 1934), p. 199, pl. 31, fig. 4 (Upper Cretaceous, Hodgeman County, Kansas, USA).

Rotalipora montsalvensis (Mornod, 1950), p. 584, fig. 4(1) (upper Cenomanian, Ruisseau des Covayes, southern east slope of the Montsalvens chain, north of Cerniat, Préalpes fribourgeoises, Switzerland).

Remarks. This study supports previous interpretation that *R. montsalvensis* is the ancestor species of *R. cushmani* (González-Donoso *et al.* 2007; Petrizzo & Gilardoni, 2020) as transitional specimens between the two species were observed.

Rotalipora praemontsalvensis Ion (1976), pp. 43–4, figs 1–4 (middle Cenomanian, Western Carpathians, Romania).

Genus *Thalmaninella* Sigal (1948).

Type species: *Thalmaninella brotzeni* Sigal (1948), p. 102, pl. 1, fig. 5.

Thalmaninella brotzeni Sigal (1948), p. 102, pl. 1, fig. 5 (middle Cenomanian, Sidi Aïssa, Algeria).

Remarks. Considered a junior synonym of *Th. globotruncanoides* for a long time (Robaszynski & Caron, 1995; Gale *et al.* 1996; Ando & Huber, 2007; González-Donoso *et al.* 2007; Lipson-Benitah, 2008; Robaszynski *et al.* 2008) until Caron & Premoli Silva (2007) and Petrizzo *et al.* (2015) demonstrated they are two distinct species.

Thalmaninella deecke (Franke, 1925), pp. 88–90, pl. 8, fig. 7 (Cenomanian, Jordanshutte auf Wollin, Pommern, Germany).

Thalmaninella gandolfii (Luterbacher & Premoli Silva, 1962), p. 267, pl. 19, fig. 3 (Gorge of the Breggia River, Canton Ticino, southeastern Switzerland).

Thalmaninella globotruncanoides Sigal (1948), p. 100, pl. 1, fig. 4 (middle Cenomanian, Sidi Aïssa, Algeria).

Remarks. The description of the species was emended in Petrizzo *et al.* (2015).

Thalmaninella micheli (Sagal & Debourle, 1957), p. 58, pl. 25, figs 4–5 (Upper Cretaceous, Bidache, Aquitaine, France).

Thalmaninella reicheli (Mornod, 1950), p. 583, fig. 5(4) (upper Cenomanian, Ruisseau des Covayes, southern east slope of the Montsalvens chain, north of Cerniat, Préalpes fribourgeoises, Switzerland).

Remarks. Neotype described and illustrated by Caron and Spezzaferri (2006).

Genus *Whiteinella* Pessagno (1967).

Type species: *Whiteinella archaeocretacea* Pessagno (1967), pp. 298–9, pl. 51, figs 22–24.

Whiteinella aumalensis (Sigal, 1952), p. 28, fig. 29 (middle Cenomanian, probably Aumale, southeast of Algiers, northern Algeria).

Whiteinella aprica (Loeblich & Tappan, 1961), p. 292, pl. 4, fig. 16 (Cenomanian, US Highway 80, west of Dallas, Texas).

Whiteinella baltica Douglas and Rankin (1969), p. 193, pl. 9, figs A–C (lower Santonian, east of Bavnodde Pynt, Bornholm, Denmark).

Whiteinella brittonensis (Loeblich & Tappan, 1961), p. 274, pl. 4, fig. 1 (Cenomanian, Eagle Ford Group, west of Cedar Hills, Dallas County, Texas).

Whiteinella paradubia (Sigal, 1952), p. 28, fig. 28 (Cenomanian, probably northern Algeria).

Supplementary material. To view supplementary material for this article, please visit <https://doi.org/10.1017/S0016756822000991>

Acknowledgements. MRP acknowledges financial support by the Italian Ministry of University and Research (MUR) ‘Dipartimenti di Eccellenza 2018–2022, Le Geoscienze per la Società: Risorse e loro evoluzione’. S Crespi is thanked for assistance at the SEM. Open Access funding provided by the Università degli Studi di Milano within the CRUI-CARE Agreement. We thank the editor B Van de Schootbrugge, HC Jenkyns and an anonymous reviewer for their careful revisions and thoughtful comments and suggestions that greatly improved the quality of this manuscript. WJ Kennedy is warmly thanked for his useful comments on an earlier version of the manuscript.

Conflict of interest. None.

References

- Abramovich S, Keller G, Stüben D and Berner Z (2003) Characterization of late Campanian and Maastrichtian planktonic foraminiferal depth habitats and vital activities based on stable isotopes. *Palaeogeography, Palaeoclimatology, Palaeoecology* **202**, 1–29.
- Anderson T F and Arthur MA (1983) Stable isotopes of oxygen and carbon and their application to sedimentologic and paleoenvironmental problems. In *Stable Isotopes in Sedimentary Geology* (eds MA Arthur, TF Anderson, IR Kaplan, J Vizier and LS Land), pp. 1–151. SEPM Short Course Notes no. 10.
- Ando A and Huber BT (2007) Taxonomic revision of the late Cenomanian planktonic foraminifera *Rotalipora greenhornensis* (Morrow, 1934). *Journal of Foraminiferal Research* **37**, 160–74.
- Ando A, Huber BT and MacLeod KG (2010) Depth-habitat reorganization of planktonic foraminifera across the Albian/Cenomanian boundary. *Paleobiology* **36**, 357–73.
- Ando A, Huber BT, MacLeod KG, Ohta T and Khim BK (2009) Blake Nose stable isotopic evidence against the mid-Cenomanian glaciation hypothesis. *Geology* **37**, 451–4.
- Ando A, Huber BT, MacLeod KG and Watkins DK (2015) Early Cenomanian “hot greenhouse” revealed by oxygen isotope record of exceptionally well-preserved foraminifera from Tanzania. *Paleoceanography* **30**, 1556–72.
- Barr FT (1962) Upper Cretaceous planktonic foraminifera from the Isle of Wight, England. *Palaeontology* **4**, 552–80.
- Batenburg SJ, de Vleeschouwer D, Sprovieri M, Hilgen FJ, Gale AS, Singer BS, Koeberl C, Coccioni R, Claeys P and Montinari A (2016) Orbital control on the timing of oceanic anoxia in the Late Cretaceous. *Climates of the Past Discussion* **12**. doi: [10.5194/cp-2015-182](https://doi.org/10.5194/cp-2015-182).
- Beil S, Kuhnt W, Holbourn AE, Aquit M, Flögel S, Chellai EH and Jabour H (2018) New insights into Cenomanian paleoceanography and climate evolution from the Tarfaya Basin, southern Morocco. *Cretaceous Research* **84**, 451–73.
- Bellier JP, Moullade M and Huber BT (2000) Mid-Cretaceous planktonic foraminifera from Blake Nose: revised biostratigraphic framework. In *Proceedings of the Ocean Drilling Program, Scientific Results, vol. 171B* (eds D Kroon, RD Norris and A Klaus), pp. 1–12. 171B. College Station, Texas.
- Bermudez PJ (1952) Estudio sistemático de los foraminíferos rotaliformes. *Boletín de Geología, Venezuela* **2**, 1–230.
- Bolli HM (1945) Zur Stratigraphie der oberen Kreide in den höheren helvetischen Decken. *Eclogae Geologicae Helveticae* **37**, 217–328.
- Bolli HM (1959) Planktonic foraminifera from the Cretaceous of Trinidad, B. W. I. *Bulletins of American Paleontology* **39**, 253–77.
- Bornemann A and Norris RD (2007) Size-related stable isotope changes in Late Cretaceous planktic foraminifera: implications for paleoecology and photosymbiosis. *Marine Micropaleontology* **65**, 32–42. doi: [10.1016/j.marmicro.2007.05.005](https://doi.org/10.1016/j.marmicro.2007.05.005).
- BouDagher-Fadel MK, Banner FT, Whittaker JE and Simmons MD (1997) *The Early Evolutionary History of Planktonic Foraminifera*. Cambridge: Chapman and Hall, 269 pp.
- Brotzen F (1942) *Die Foraminiferengattung Gavelinella nov. gen. und die Systematik der Rotaliformes*. Stockholm: Sveriges Geologiska Undersökning **36(8) C** (451), 1–60.
- Caron M (1966) Globotruncanoidae du Crétacé supérieur du synclinal de la Grayère (Préalpes médianes, Suisse). *Revue de Micropaléontologie* **9**, 69–93.
- Caron M and Premoli Silva I (2007) New description of the rotaliporid species *brotzeni* and *globotruncanoides* Sigal, 1948 based on re-examination of type material. *Rivista Italiana di Paleontologia e Stratigrafia* **113**, 525–30.
- Caron M and Spezzaferri S (2006) Scanning electron microscope documentation of the lost holotypes of Mornod, 1949: *Thalmaninella reicheli* and *Rotalipora montsalvensis*. *Journal of Foraminiferal Research* **36**, 374–8.
- Carsey DO (1926) Foraminifera of the Cretaceous of Central Texas. *University of Texas Bulletin* **2612**, 1–56.
- Carter DJ and Hart MB (1977) Aspects of mid-Cretaceous stratigraphical micropalaeontology. *Bulletin of the British Museum of Natural History (Geology)* **29**, 1–135.
- Coccioni R and Galeotti S (2003) The Mid-Cenomanian Event: prelude to OAE 2. *Palaeogeography, Palaeoclimatology, Palaeoecology* **190**, 427–40.
- Cushman JA (1938) Cretaceous species of *Guembelina* and related genera. *Contributions from the Cushman Laboratory for Foraminiferal Research* **14**, 2–28.
- Denne RA, Hinote RE, Breyer JA, Kosanke TH, Lees JA, Engelhardt-Moore N, Spaw JM and Tur N (2014) The Cenomanian–Turonian Eagle Ford Group of South Texas: insights on timing and paleoceanographic conditions from geochemistry and micropaleontologic analyses. *Palaeogeography, Palaeoclimatology, Palaeoecology* **413**, 2–28.
- Desmares D, Grosheny D and Beauvoisin B (2008) Ontogeny and phylogeny of upper Cenomanian rotaliporids (Foraminifera). *Marine Micropaleontology* **69**, 91–105.
- Ditchfield P and Marshall JD (1989) Isotopic variation in rhythmically bedded chalks: paleotemperature variation in the Upper Cretaceous. *Geology* **17**, 842–5.
- Douglas RG (1969) Upper Cretaceous planktonic foraminifera in northern California. *Micropaleontology* **15**, 151–209.
- Douglas RG and Rankin C (1969) Cretaceous planktonic foraminifera from Bornholm and their zoogeographic significance. *Lethaia* **2**, 185–217.
- Du Vivier ADC, Selby D, Condon D J, Takashima R and Nishi H (2015) Pacific $^{187}\text{Os}/^{188}\text{Os}$ isotopic chemistry and U–Pb geochronology: synchronicity of global Os isotope change across OAE 2. *Earth and Planetary Science Letters* **428**, 204–16.
- Du Vivier ADC, Selby D, Sageman BB, Jarvis I, Gröcke DR and Voigt S (2014) Marine $^{187}\text{Os}/^{188}\text{Os}$ isotope stratigraphy reveals the interaction of volcanism and ocean circulation during Oceanic Anoxic Event 2. *Earth and Planetary Science Letters* **389**, 23–33.
- Dubicka Z and Machalski M (2017) Foraminiferal record in a condensed marine succession: a case study from the Albian and Cenomanian (mid-Cretaceous) of Annapol, Poland. *Geological Magazine* **154**, 399–418.
- Eicher DL and Worstell P (1970) Cenomanian and Turonian foraminifera from the Great Plains, United States. *Micropaleontology* **16**, 269–324.
- Eldrett JS, Ma C, Bergman SC, Lutz B, Gregory FJ, Dodsworth P, Phipps M, Hardas P, Minisini D, Ozkan A, Ramezani J, Bowring SA, Kamo SL, Ferguson K, Macaulay C and Kelly AE (2015) An astronomically calibrated stratigraphy of the Cenomanian, Turonian and earliest Coniacian from the

- Cretaceous Western Interior Seaway, USA: implications for global chronostratigraphy. *Cretaceous Research* **56**, 316–44.
- Erbacher J, Bornemann A, Petrizzo MR and Huck S** (2020) Chemostratigraphy and stratigraphic distribution of keeled planktonic foraminifera in the Cenomanian of the North German Basin. *Zeitschrift der Deutschen Gesellschaft für Geowissenschaften (Int. J. Reg. Geol.), Karl-Armin Tröger Memorial Issue* **171**, 149–61. doi: [10.1127/zdgg/2020/0211](https://doi.org/10.1127/zdgg/2020/0211).
- Erbacher J and Thurow J** (1997) Influence of oceanic anoxic events on the evolution of mid-Cretaceous radiolaria in the North Atlantic and western Tethys. *Marine Micropaleontology* **30**, 139–58.
- Erbacher J, Thurow J and Littke R** (1996) Evolution patterns of radiolaria and organic matter variations: a new approach to identify sea-level changes in mid-Cretaceous pelagic environments. *Geology* **24**, 499–502.
- Falzone F and Petrizzo MR** (2020) Patterns of planktonic foraminiferal extinctions and eclipses during Oceanic Anoxic Event 2 at Eastbourne (SE England) and other mid low latitude locations. *Cretaceous Research* **116**, 104593. doi: [10.1016/j.cretres.2020.104593](https://doi.org/10.1016/j.cretres.2020.104593).
- Falzone F and Petrizzo MR** (2022) Evidence for changes in sea-surface circulation patterns and ~20° equatorward expansion of the Boreal bioprovince during a cold snap of Oceanic Anoxic Event 2 (Late Cretaceous). *Global and Planetary Change* **208**, 103678.
- Falzone F, Petrizzo MR, Caron M, Leckie RM and Elderbak K** (2018) Age and synchronicity of planktonic foraminiferal bioevents across the Cenomanian–Turonian boundary interval (Late Cretaceous). *Newsletters on Stratigraphy* **51**, 343–80.
- Falzone F, Petrizzo MR, Jenkyns HC and Gale AS** (2016) Planktonic foraminiferal biostratigraphy and assemblage composition across the Cenomanian–Turonian boundary interval at Clot Chevalier (Vocontian Basin, SE France). *Cretaceous Research* **59**, 69–97.
- Falzone F, Petrizzo MR, MacLeod KG and Huber BT** (2013) Santonian–Campanian planktonic foraminifera from Tanzania, Shatsky Rise and Exmouth Plateau: species depth ecology and paleoceanographic inferences. *Marine Micropaleontology* **103**, 15–29. doi: [10.1016/j.marmicro.2013.07.003](https://doi.org/10.1016/j.marmicro.2013.07.003).
- Fraass AJ, Kelly DC and Peters SE** (2015) Macroevolutionary history of the planktic foraminifera. *Annual Review of Earth and Planetary Sciences* **43**, 139–66.
- Franke A** (1925) Die Foraminiferen der pommerschen Kriede. *Abhandlungen aus dem Geologisch-Paläontologischen Institut der Universität Greifswald* **6**, 1–96.
- Friedrich O, Erbacher J, Wilson PA, Moriya K and Mutterlose J** (2009) Paleoenvironmental changes across the Mid Cenomanian Event in the tropical Atlantic Ocean (Demerara Rise, ODP Leg 207) inferred from benthic foraminiferal assemblages. *Marine Micropaleontology* **71**, 28–40.
- Gale AS** (1989) Field meeting at Folkestone Warren, 29th November, 1987. *Proceedings of the Geologists' Association* **100**, 73–82.
- Gale AS** (1990) A Milankovitch scale for Cenomanian time. *Terra Nova* **1**, 420–5.
- Gale AS** (1995) Cyclostratigraphy and correlation of the Cenomanian stage in Western Europe. In *Orbital Forcing Timescales and Cyclostratigraphy* (ed. MR House), pp. 177–97. *Geological Society of London, Special Publication no. 85*, 177–97.
- Gale AS and Christensen WK** (1996) Occurrence of the belemnite *Actinocamax plenus* in the Cenomanian of SE France and its significance. *Bulletin of the Geological Society of Denmark* **43**, 68–77.
- Gale AS, Hancock JM and Kennedy WJ** (1999) Biostratigraphical and sequence correlation of the Cenomanian successions in Mangyshlak (W. Kazakhstan) and Crimea (Ukraine) with those in southern England. *Bulletin de l'Institut Royal des Sciences Naturelles de Belgique, Sciences de la Terre* **69** (SUPPL. A), 67–86.
- Gale AS, Jenkyns HC, Tsikos H, van Breugel Y, Sinnighe Damsté JS, Bottini C, Erba E, Russo F, Falzone F, Petrizzo MR, Dickson AJ and Wray DS** (2019a) High-resolution bio- and chemostratigraphy of an expanded record of Oceanic Anoxic Event 2 (Late Cenomanian–Early Turonian) at Clot Chevalier, near Barre, SE France (Vocontian Basin, SE France). *Newsletters on Stratigraphy* **52**, 97–129. doi: [10.1127/nos/2018/0445](https://doi.org/10.1127/nos/2018/0445).
- Gale AS, Kennedy WJ and Walaszczyk I** (2019b) Upper Albian, Cenomanian and lower Turonian stratigraphy, ammonite and inoceramid bivalve faunas from the Cauvery Basin, Tamil Nadu, South India. *Acta Geologica Polonica* **69**, 161–338.
- Gale AS and Kennedy WJ** (2021) Condensation and channelling in Cenomanian chalks of the northern Anglo-Paris Basin: the Totternhoe Stone and related deposits. *Newsletters on Stratigraphy* **55**, 231–54.
- Gale AS, Kennedy WJ, Burnett JA, Caron M and Kidd BE** (1996) The Late Albian to early Cenomanian succession at Mont Risou near Rosans (Drôme, SE France): an integrated study (ammonites, inoceramids, planktonic foraminifera, nannofossils, oxygen and carbon isotopes). *Cretaceous Research* **17**, 515–606.
- Gale AS, Mutterlose J, Batenburg S, Gradstein FM, Agterberg FP, Ogg JG and Petrizzo MR** (2020) The Cretaceous period. In *Geologic Time Scale 2020*, vol. 2 (eds FM Gradstein, JG Ogg, MD Schmitz and GM Ogg), pp. 1023–86. Amsterdam: Elsevier B.V. doi: [10.1016/B978-0-12-824360-2.00027-9](https://doi.org/10.1016/B978-0-12-824360-2.00027-9).
- Gale AS, Voigt S, Sageman BB and Kennedy WJ** (2008) Eustatic sea-level record for the Cenomanian (Late Cretaceous): extension to the Western Interior Basin, USA. *Geology* **36**, 859–62.
- Gale AS, Young J, Shackleton NJ, Crowhurst SJ and Wray DS** (1999) Orbital tuning of Cenomanian marly chalk successions: towards a Milankovitch time-scale for the Late Cretaceous. *Philosophical Transactions of the Royal Society, London, A*, **357**, 1815–29.
- Gambacorta G, Jenkyns HC, Russo F, Tsikos H, Wilson PA, Faucher G and Erba E** (2015) Carbon- and oxygen-isotope records of mid-Cretaceous Tethyan pelagic sequences from the Umbria-Marche and Belluno Basins (Italy). *Newsletters on Stratigraphy* **48**, 299–323.
- Gandolfi R** (1942) Ricerche micropaleontologiche e stratigrafiche sulla Scaglia e sui Flysch cretaccici dei dintorni di Balerna. *Rivista Italiana di Paleontologia, Memorie* **4**, 1–118.
- Georgescu MD** (2009) Upper Albian–lower Turonian non-schackoinid planktic foraminifera with elongate chambers: morphology reevaluation, taxonomy and evolutionary classification. *Revista Española de Micropaleontología* **41**, 255–94.
- Georgescu MD and Huber BT** (2009) Early evolution of the Cretaceous serial planktic foraminifera (late Albian–Cenomanian). *Journal of Foraminiferal Research* **39**, 335–60.
- Gertsch B, Adatte T, Keller G, Tantaw AAA, Berner Z, Mort HP and Fleitmann D** (2010) Middle and late Cenomanian oceanic anoxic events in shallow and deeper shelf environments of western Morocco. *Sedimentology* **57**, 1430–62.
- Giorgioni M, Weissert H, Bernasconi SM, Hochuli PA, Keller CE, Coccioni R, Petrizzo MR, Lukeneder A and Garcia TI** (2015) Paleoclimatological changes during the Albian–Cenomanian in the Tethys and North Atlantic and the onset of the Cretaceous chalk. *Global and Planetary Change* **126**, 46–61.
- Giraud F, Reboulet S, Deconinck JF, Martinez M, Carpentier A and Bréziat C** (2013) The Mid-Cenomanian Event in southeastern France: evidence from palaeontological and clay mineralogical data. *Cretaceous Research* **46**, 43–58.
- González-Donoso JM, Linares D and Robaszynski F** (2007) The rotaliporids, a polyphyletic group of Albian–Cenomanian planktonic foraminifera: emendation of genera. *Journal of Foraminiferal Research* **37**, 175–86.
- Gradstein FM, Ogg JG, Schmitz MD and Ogg GM** (2012) *The Geologic Time Scale 2012*. Oxford: Elsevier, 1144 pp.
- Gradstein FM, Ogg JG, Schmitz MD and Ogg GM** (2020) *Geologic Time Scale 2020*. Oxford: Elsevier, 1300 pp.
- Gradstein FM, Ogg JG and Smith AG** (2004) *A Geological Time Scale 2004*. Cambridge: Cambridge University Press, 589 pp.
- Hardas P, Mutterlose J, Friedrich O and Erbacher J** (2012) The Middle Cenomanian Event in the equatorial Atlantic: the calcareous nannofossil and benthic foraminiferal response. *Marine Micropaleontology* **96**, 66–74.
- Hart MB** (1999) The evolution and biodiversity of Cretaceous Foraminiferida. *Geobios* **32**, 247–55. doi: [10.1016/S0016-6995\(99\)80038-2](https://doi.org/10.1016/S0016-6995(99)80038-2).
- Hart MB, Bailey HW, Crittenden S, Fletcher BN, Price R and Sweicicki A** (1989) *Cretaceous*. In *Stratigraphic Atlas of Fossil Foraminifera, 2nd edn* (eds DG Jenkins and JW Murray), pp. 273–371. British Micropaleontological Society Series. Chichester: John Wiley & Sons.

- Hasegawa T (1999) Planktonic foraminifera and biochronology of the Cenomanian-Turonian (Cretaceous) sequence in the Oyubari area, Hokkaido, Japan. *Paleontological Research* **3**, 173–92.
- Hermes JJ (1969) Late Albian foraminifera from the Subbetic of Southern Spain. *Geologie en Mijnbouw* **48**, 35–65.
- Huber BT and Leckie RM (2011) Planktic foraminiferal species turnover across deep-sea Aptian/Albian boundary sections. *Journal of Foraminiferal Research* **41**, 53–95.
- Huber BT, Leckie RM, Norris R D, Bralower TJ and CoBabe E (1999) Foraminiferal assemblage and stable isotopic change across the Cenomanian–Turonian boundary in the subtropical North Atlantic. *Journal of Foraminiferal Research* **29**, 392–417.
- Huber BT, Petrizzo MR and Falzoni F (2022) Taxonomy and phylogeny of Albian–Maastrichtian planispiral planktonic foraminifera traditionally assigned to *Globigerinelloides*. *Micropaleontology* **68**, 117–83.
- Huber BT, Petrizzo MR, Young JR, Falzoni F, Gilardoni SE, Bown PR and Wade BS (2016) Pforams@ mikrotax. A new online taxonomic database for planktonic foraminifera. *Micropaleontology* **62**, 429–38.
- Ion J (1976) A propos de la souche des Rotalipores, *Rotalipora praemontsalvensis* n. sp.: Dari de Seama ale Sedintelor. *Institutul de Geologie si Geofizica Bucharest* **62**, 39–46.
- Jacob K and Sastry MVA (1950) On the occurrence of *Globotruncana* in Uttatur stage of the Trichinopoly Cretaceous, South India. *Science and Culture* **16**, 266–8.
- Jarvis I, Gale AS, Jenkyns HC and Pearce MA (2006) Secular variation in Late Cretaceous carbon isotopes: a new $\delta^{13}\text{C}$ carbonate reference curve for the Cenomanian–Campanian (99.6–70.6 Ma). *Geological Magazine* **143**, 561–608.
- Jarvis I, Lignum JS, Gröcke DR, Jenkyns HC and Pearce MA (2011) Black shale deposition, atmospheric CO_2 drawdown, and cooling during the Cenomanian–Turonian Oceanic Anoxic Event. *Paleoceanography* **26**, PA3201. doi: [10.1029/2010PA002081](https://doi.org/10.1029/2010PA002081).
- Jarvis I, Murphy AM and Gale AS (2001) Geochemistry of pelagic and hemipelagic carbonates: criteria for identifying systems tracts and sea-level changes. *Journal of the Geological Society of London* **158**, 685–96.
- Jefferies RPS (1962) The palaeoecology of the *Actinocamax plenus* subzone (lowest Turonian) in the Anglo-Paris Basin. *Palaeontology* **4**, 609–47.
- Jefferies RPS (1963) The stratigraphy of the *Actinocamax plenus* subzone (Turonian) in the Anglo-Paris Basin. *Proceedings of the Geologists' Association* **74**, 1–33.
- Jenkyns HC (2010) Geochemistry of oceanic anoxic events. *Geochemistry, Geophysics, Geosystems* **11**, Q03004, doi: [10.1029/2009GC002788](https://doi.org/10.1029/2009GC002788).
- Jenkyns HC, Dickson AJ, Ruhl M and van den Boorn SH (2017) Basalt-seawater interaction, the Plenus Cold Event, enhanced weathering and geochemical change: deconstructing Oceanic Anoxic Event 2 (Cenomanian–Turonian, Late Cretaceous). *Sedimentology* **64**, 16–43.
- Jiménez Berrocso Á, MacLeod K, Martin E, Bourbon E, Londoño C and Basak C (2010) Nutrient trap for Late Cretaceous organic-rich black shales in the tropical North Atlantic. *Geology* **38**, 1111–4, doi: [10.1130/G31195.1](https://doi.org/10.1130/G31195.1).
- Joo YJ and Sageman BB (2014) Cenomanian to Campanian carbon isotope chemostratigraphy from the Western Interior Basin, USA. *Journal of Sedimentary Research* **84**, 529–42.
- Kennedy WJ (1969) The correlation of the Lower Chalk of south-east England. *Proceedings of the Geologists' Association* **80**, 459–560.
- Kennedy WJ, Gale AS, Bown PR, Caron M, Davey RJ, Gröcke D and Wray DS (2000) Integrated stratigraphy across the Aptian–Albian boundary in the Marnes Bleues, at the Col de Pré-Guittard, Arnavon (Drome) and at Tartonne (Alpes de Haute Provence), France: a candidate Global Boundary Stratotype Section and Boundary Point for the base of the Albian Stage. *Cretaceous Research* **21**, 591–720.
- Kennedy WJ, Gale AS, Huber BT, Petrizzo MR, Bown P, Barchetta A and Jenkyns HC (2014) Integrated stratigraphy across the Aptian/Albian boundary at Col de Pré-Guittard (southeast France): a candidate global boundary stratotype section. *Cretaceous Research* **51**, 248–59.
- Klaus J (1960) Étude biométrique et statistique de quelques espèces de Globotruncanidés 1. Les espèces du genre *Praeglobotruncana* dans le Cénomanien de la Breggia (Tessin, Suisse méridionale). *Eclogae Geologicae Helvetiae* **53**, 285–308.
- Kuhnt W, Holbourn A, Gale AS, Chellai EH and Kennedy WJ (2009) Cenomanian sequence stratigraphy and sea-level fluctuations in the Tarfaya Basin (SW Morocco). *Geological Society of America Bulletin* **121**, 1695–710.
- Leckie RM (1987) Paleocology of mid-Cretaceous planktonic foraminifera; a comparison of open ocean and epicontinental sea assemblages. *Micropaleontology* **33**, 164–76. doi: [10.2307/1485491](https://doi.org/10.2307/1485491).
- Leckie RM, Bralower TJ and Cashman R (2002) Oceanic anoxic events and plankton evolution: biotic response to tectonic forcing during the mid-Cretaceous. *Paleoceanography* **17**. doi: [10.1029/2001PA000623](https://doi.org/10.1029/2001PA000623).
- Leckie RM, Yuretrich RF, West OLO, Finkelstein D and Schmidt M (1998) Paleocyanography of the southwestern Western Interior Sea during the time of the Cenomanian–Turonian boundary (Late Cretaceous). In *Stratigraphy and Paleoenvironments of the Cretaceous Western Interior Seaway* (eds W Dean & MA Arthur), pp. 101–26. SEPM, Concepts in Sedimentology and Paleontology, vol. 6.
- Li X, Jenkyns HC, Wang C, Hu X, Chen X, Wei Y, Huang Y and Cui J (2006) Upper Cretaceous carbon- and oxygen-isotope stratigraphy of hemipelagic carbonate facies from southern Tibet, China. *Journal of the Geological Society* **163**, 375–82.
- Lipson-Benitah S (2008) Phylogeny of the Middle Cretaceous (late Albian-late Cenomanian) planktonic foraminiferal genera *Parathalmanninella* nov. gen. and *Thalmanninella*. *Journal of Foraminiferal Research* **38**, 183–9.
- Lipson-Benitah S, Almogi-Labin A and Sass E (1997) Cenomanian biostratigraphy and palaeoenvironments in the north west Carmel region, northern Israel. *Cretaceous Research* **18**, 469–91.
- Loeblich AR and Tappan H (1961) Cretaceous planktonic foraminifera, 1 – Cenomanian. *Micropaleontology* **7**, 257–304.
- Luterbacher HP and Premoli Silva I (1962) Note préliminaire sur une révision du profil de Gubbio, Italie. *Rivista Italiana di Paleontologia e Stratigrafia* **68**, 253–88.
- Ma C, Hinnov LA, Eldrett JS, Meyers SR, Bergman SC, Minisini D and Lutz B. (2022) Centennial to millennial variability of greenhouse climate across the mid-Cenomanian event. *Geology* **50**, 227–231.
- MacLeod KG, Martin EE and Blair SW (2008) Nd isotopic excursion across Cretaceous ocean anoxic event 2 (Cenomanian–Turonian) in the tropical North Atlantic. *Geology* **36**, 811–14.
- Magné J and Sigal J (1954) Description des espèces nouvelles: 1 – Foraminifères. *Bulletin de la Société Géologique de France* **3/6**, 471–91.
- Martin EE, MacLeod KG, Jiménez Berrocso A and Bourbon E (2012) Water mass circulation on Demerara Rise during the Late Cretaceous based on Nd isotopes. *Earth and Planetary Science Letters* **327–328**, 111–20.
- Miller KG, Kominz MA, Browning JV, Wright JD, Mountain GS, Katz ME, Sugarman PJ, Cramer BS, Christie-Blick N and Pekar SF (2005) The Phanerozoic record of global sea-level change. *Science* **310**, 1293–8.
- Miller KG, Sugarman PJ, Browning JV, Kominz MA, Hernández JC, Olsson RK, Wright JD, Feigenson MD and Van Sickle W (2003) Late Cretaceous chronology of large, rapid sea-level changes: glacioeustasy during the greenhouse world. *Geology* **31**, 585–8.
- Mitchell SF and Carr IT (1998) Foraminiferal response to mid-Cenomanian (Upper Cretaceous) palaeoceanographic events in the Anglo-Paris Basin (Northwest Europe). *Palaeogeography, Palaeoclimatology, Palaeoecology* **137**, 103–25.
- Mitchell SF, Paul CRC and Gale AS (1996) Carbon isotopes and sequence stratigraphy. In *High Resolution Sequence Stratigraphy: Innovations and Applications* (eds J Howell & JF Aitken), pp. 11–24. *Geological Society of London, Special Publication no. 104*.
- Moghadam HV and Paul CRC (2000) Micropalaeontology of the Cenomanian at Chinnor, Oxfordshire, and comparison with the Dover-Folkestone succession. *Proceedings of the Geologists' Association* **111**, 17–39.
- Moriya K, Wilson PA, Friedrich O, Erbacher J and Kawahata H (2007) Testing for ice sheets during the mid-Cretaceous greenhouse using glassy foraminiferal calcite from the mid-Cenomanian tropics on Demerara Rise. *Geology* **35**, 615–8.
- Mornod AL (1950) Les Globotrotalides du Crétacé supérieur du Montsalvens (Préalpes fribourgeoises). *Eclogae Geologicae Helvetiae* **42**, 573–95.
- Morrow AL (1934) Foraminifera and Ostracoda from the Upper Cretaceous of Kansas. *Journal of Paleontology* **8**, 186–205.

- Norris RD and Wilson PA (1998) Low-latitude sea-surface temperatures for the mid- Cretaceous and the evolution of planktic foraminifera. *Geology* **26**, 823–6.
- O'Connor LK, Rimmelzwaal S, Robinson SA, Batenburg SJ, Jenkyns HC, Parkinson I and Gale AS (2019) Deconstructing the Plenus Cold Event (Cenomanian, Cretaceous). *Paleoceanography and Palaeoclimatology* **35**. doi: 10.1029/2019PA003631.
- Ogg JG, Ogg GM and Gradstein FM (2016) *A Concise Geologic Time Scale: 2016*. Amsterdam: Elsevier, 240 pp.
- Paul CRC, Mitchell SF, Marshal JD, Leary PN, Gale AS, Duane AM and Ditchfield PW (1994) Paleocceanographic events in the middle Cenomanian of Northwest Europe. *Cretaceous Research* **15**, 707–38.
- Peryt D (1983) Planktonic foraminiferal zonation of Mid-Cretaceous of the Annopol Anticline (central Poland). *Zitteliana* **10**, 575–83.
- Pessagno EA Jr (1960) Stratigraphy and micropaleontology of the Cretaceous and lower Tertiary of Puerto Rico. *Micropaleontology* **6**, 87–110.
- Pessagno EA Jr (1967) Upper Cretaceous planktonic foraminifera from the western Gulf Coastal Plain. *Paleontographica Americana* **5**, 245–445.
- Pessagno EA Jr (1969) Upper Cretaceous stratigraphy of the western Gulf Coast area of Mexico, Texas, and Arkansas. *Geological Society of America Memoir* **111**, 139 pp.
- Petrizzo MR, Amaglio G, Watkins DK, MacLeod KG, Huber BT, Hasegawa T and Wolfgring E (2022a) Biotic and paleoceanographic changes across the Late Cretaceous Oceanic Anoxic Event 2 in the southern high latitudes (IODP sites U1513 and U1516, SE Indian Ocean). *Paleoceanography and Paleoclimatology*, **37**, e2022PA004474.
- Petrizzo MR, Caron M and Premoli Silva I (2015) Remarks on the identification of the Albian/Cenomanian boundary and taxonomic clarification of the planktonic foraminifera index species *globotruncanoides*, *brotzenii* and *tehamaensis*. *Geological Magazine* **152**, 521–36.
- Petrizzo MR, MacLeod KG, Watkins DK, Wolfgring E and Huber BT (2022b) Late Cretaceous paleoceanographic evolution and the onset of cooling in the Santonian at southern high latitudes (IODP Site U1513, SE Indian Ocean). *Paleoceanography and Paleoclimatology* **37**, e2021PA004353.
- Petrizzo MR and Gilardoni SE (2020) Planktonic foraminiferal biostratigraphy of late Albian-Cenomanian pelagic sequences from the Umbria-Marche basin (central Italy) and the Mazagan Plateau (northeast Atlantic Ocean). *Rivista Italiana di Paleontologia e Stratigrafia* **126**, 865–904.
- Petrizzo MR and Huber BT (2006) Biostratigraphy and taxonomy of late Albian planktonic foraminifera from ODP Leg 171b (Western North Atlantic Ocean). *Journal of Foraminiferal Research* **36**, 166–90.
- Petrizzo MR, Huber BT, Falzoni F and MacLeod KG (2020) Changes in biogeographic distribution patterns of southern mid-to high latitude planktonic foraminifera during the Late Cretaceous hot to cool greenhouse climate transition. *Cretaceous Research* **104547**. doi: 10.1016/j.cretres.2020.104547.
- Petrizzo MR, Huber BT, Gale AS, Barchetta A and Jenkyns HC (2012) Abrupt planktic foraminiferal turnover across the Niveau Kilian at Col de Pré-Guittard (Vocontian Basin, southeast France): new criteria for defining the Aptian/Albian boundary. *Newsletters on Stratigraphy* **45**, 55–74.
- Petrizzo MR, Huber BT, Gale AS, Barchetta A and Jenkyns HC (2013) Erratum: Abrupt planktic foraminiferal turnover across the Niveau Kilian at Col de Pré-Guittard (Vocontian Basin, southeast France): new criteria for defining the Aptian/Albian boundary. *Newsletters on Stratigraphy* **46**, 93.
- Petrizzo MR, Huber BT, Wilson PA and MacLeod KG (2008) Late Albian paleoceanography of the western subtropical North Atlantic. *Paleoceanography* **23**, 1.
- Petrizzo MR, Jiménez Berrocoso A, Falzoni F, Huber BT and MacLeod KG (2017) The Coniacian–Santonian sedimentary record in southern Tanzania (Ruvuma Basin, East Africa): planktonic foraminiferal evolutionary, geochemical and paleoceanographic patterns. *Sedimentology*, **64**, 252–85. doi: 10.1111/sed.12331.
- Petrizzo MR, Watkins DK, MacLeod KG, Hasegawa T, Huber BT, Batenburg SJ and Kato T (2021) Exploring the paleoceanographic changes registered by planktonic foraminifera across the Cenomanian-Turonian boundary interval and Oceanic Anoxic Event 2 at southern high latitudes in the Mentelle Basin (SE Indian Ocean). *Global and Planetary Change* **206**, 103595. doi: 10.1016/j.gloplacha.2021.103595.
- Plummer HJ (1931) Some Cretaceous foraminifera in Texas. *University of Texas Bulletin* **101**, 109–203.
- Porthault B (1970) Le Sénonien inférieur de Puget-Théniers (Alpes-Maritimes) et sa microfaune. *Geobios* **3**, 41–106.
- Premoli Silva I and Sliter WV (1995) Cretaceous planktonic foraminiferal biostratigraphy and evolutionary trends from the Bottaccione section, Gubbio, Italy. *Paleontographia Italica* **82**, 1–89.
- Premoli Silva I and Sliter WV (1999) Cretaceous paleoceanography: evidence from planktonic foraminiferal evolution. In *The Evolution of the Cretaceous Ocean-Climate System* (eds E Barrera & CC Johnson), pp.301–28. Boulder, Colorado: Geological Society of America, Special Paper no. 332.
- Reboullet S, Giraud F, Colombié C and Carpentier A (2013) Integrated stratigraphy of the Lower and Middle Cenomanian in a Tethyan section (Blieux, southeast France) and correlations with Boreal basins. *Cretaceous Research* **40**, 170–89.
- Reiss Z (1957) The Bilamellidea, nov. superfam., and remarks on Cretaceous globorotaliids. *Contributions from the Cushman Foundation for Foraminiferal Research* **8**, 127–45.
- Robaszynski F, Amédéo F, González-Donoso JM and Linares D (2008) The Albian (Vraconnian)-Cenomanian boundary at the western Tethyan margins (central Tunisia and southeastern France). *Bulletin de la Société géologique de France* **179**, 245–66.
- Robaszynski F and Caron M (1995) Foraminifères planctoniques du Crétacé; commentaire de la zonation Europe-Méditerranée. *Bulletin de la Société géologique de France* **166**, 681–92.
- Robaszynski F, Caron M, Amédéo F, Dupuis C, Hardenbol J, González-Donoso JM, Linares D and Gartner S (1994) Le Cénomanien de la région de Kalaat Senan (Tunisie Centrale): Litho-biostratigraphie et interprétation séquentielle. *Revue de Paléobiologie*. **12**, 351–505.
- Robaszynski F, Gale A, Juignet P, Amédéo F and Hardenbol J (1998) Sequence stratigraphy in the Upper Cretaceous series of the Anglo-Paris Basin: exemplified by the Cenomanian stage. In *Mesozoic and Cenozoic Sequence Chronostratigraphic Framework of European Basins* (eds JAN Hardenbol, J Thierry, MB Farley, T Jacquin, PC De Graciansky & PR Vail), 363–86. *SEPM Special Publication* **60**.
- Rodriguez-Lázaro J, Pascual A and Elorza J (1998) Cenomanian events in the deep western Basque Basin: the Leioa section. *Cretaceous Research* **19**, 673–700.
- Sacal V and Debourle A (1957) Foraminifères d'Aquitaine; 2^e partie, Peneroplidae a Victoriellidae. *Mémoires de la Société Géologique de France* **78**, 1–88.
- Sageman BB, Meyers SR and Arthur MA (2006) Orbital timescale for the Cenomanian-Turonian boundary stratotype and OAE II, central Colorado, USA. *Geology* **34**, 125–8.
- Scaife JD, Ruhl M, Dickson AJ, Mather TA, Jenkyns HC, Percival LME, Hesselbo SP, Cartwright J, Eldrett JS, Bergman SC and Minisini D (2017) Sedimentary mercury enrichments as a marker for submarine large igneous province volcanism? Evidence from the Mid-Cenomanian event and Oceanic Anoxic Event 2 (Late Cretaceous). *Geochemistry, Geophysics, Geosystems* **18**, 4253–75.
- Scheibnerova V (1960) Poznamky rodu *Praeglobotruncana* Bermudez y kysuckych vrstiev bradloveho pasma. *Geologicky Zbornik Geologica Carpathica* **11**, 85–90.
- Scheibnerova V (1962) Stratigrafia strednej a vrchnej kriedy tétýdnej oblasti na zaklade globotruncanid. *Geologicky Zbornik Geologica Carpathica* **13**, 219–26.
- Schiebel R and Hemleben C (2017) *Planktic foraminifers in the Modern Ocean*. Berlin and Heidelberg: Springer-Verlag GmbH, 358 pp. doi: 10.1007/978-3-662-50297-6.
- Scotese CR (2016) PALEOMAP PaleoAtlas for GPlates and the PaleoData Plotter Program. PALEOMAP Project. <http://www.earthbyte.org/paleomap-paleoatlas-for-gplates>.
- Sigal J (1948) Notes sur les genres de foraminifères Rotalipora Brotzen 1942 et Thalmanninella, famille des Globorotaliidae. *Revue de l'Institut français du Pétrole Paris*, **3**, 4.
- Sigal J (1952) Aperçu stratigraphique sur la micropaléontologie du Crétacé. *Congrès Géologique International, XIX, Monographie Régionale, Algiers 1* (Algeria), 26.

- Stoll HM and Schrag DP** (2000) High-resolution stable isotope records from the Upper Cretaceous rocks of Italy and Spain: glacial episodes in a greenhouse planet? *Geological Society of America Bulletin* **112**, 308–19.
- Stoll HM and Schrag DP** (2001) Sr/Ca variations in Cretaceous carbonates: relation to productivity and sea level changes. *Palaeogeography, Palaeoclimatology, Palaeoecology* **168**, 311–36.
- Subbotina NN** (1949) Microfauna of the Cretaceous of the southern slope of the Caucasus. *VNIGRI, Microfauna of the Oilfields of the USSR* **34**, 5–36.
- Tappan H** (1940) Foraminifera from the Grayson Formation of northern Texas. *Journal of Paleontology* **14**, 93–126.
- Trujillo EF** (1960) Upper Cretaceous Foraminifera from near Redding, Shasta County, California. *Journal of Paleontology* **34**, 290–346.
- Turgeon SC and Creaser RA** (2008) Cretaceous Anoxic Event 2 triggered by a massive magmatic episode. *Nature* **454**, 323–6.
- Voigt S, Gale AS and Flögel S** (2004) Midlatitude shelf seas in the Cenomanian–Turonian greenhouse world: temperature evolution and North Atlantic circulation. *Paleoceanography* **19**, 4. doi: [10.1029/2004PA001015](https://doi.org/10.1029/2004PA001015).
- Wendler I, Huber BT, MacLeod KG and Wendler JE** (2013) Stable oxygen and carbon isotope systematics of exquisitely preserved Turonian foraminifera from Tanzania: understanding isotopic signatures in fossils. *Marine Micropaleontology* **102**, 1–33.
- Williams-Mitchell E** (1948) The zonal value of foraminifera in the Chalk of England. *Proceedings of the Geologists' Association* **59**, 96–112.
- Wilmsen M** (2003) Sequence stratigraphy and palaeoceanography of the Cenomanian Stage in northern Germany. *Cretaceous Research* **24**, 525–68.
- Wilmsen M** (2007) Integrated stratigraphy of the upper Lower–lower Middle Cenomanian of northern Germany and southern England. *Acta Geologica Polonica* **57**, 263–79.
- Wilmsen M, Niebuhr B and Hiss M** (2005) The Cenomanian of northern Germany: facies analysis of a transgressive biosedimentary system. *Facies* **51**, 242–63.
- Wilmsen M, Wood CJ, Niebuhr B and Zawischa D** (2007) The fauna and palaeoecology of the Middle Cenomanian Praeactinocamax primus event from the type-locality (Wünstorf quarry, northern Germany). *Cretaceous Research* **28**, 428–60.
- Wilson PA, Norris RD and Cooper MJ** (2002) Testing the Cretaceous greenhouse hypothesis using glassy foraminiferal calcite from the core of the Turonian tropics on Demerara Rise. *Geology* **30**, 607–10.
- Wonders AAH** (1978) Middle and Late Cretaceous pelagic sediments of the Umbrian Sequence in the Central Apennines. *Proceedings of the Koninklijke Nederlandse Akademie Wetenschappen* **81**, 171–205.
- Wonders AAH** (1980) Middle and Late Cretaceous planktonic foraminifera of the western Mediterranean area. *Utrecht Micropaleontological Bulletins* **24**, 1–158.
- Wright CW, Kennedy WJ, Hancock JM and Gale AS** (2017) The ammonoidea of the lower chalk part 7. *Monographs of the Palaeontographical Society* **171**, 461–561.
- Zheng XY, Jenkyns HC, Gale AS, Ward DJ and Henderson, GM** (2013) Changing ocean circulation and hydrothermal inputs during Ocean Anoxic Event 2 (Cenomanian–Turonian): evidence from Nd-isotopes in the European shelf sea. *Earth and Planetary Science Letters* **375**, 338–48.
- Zheng XY, Jenkyns HC, Gale AS, Ward DJ and Henderson, GM** (2016) A climatic control on reorganization of ocean circulation during the mid-Cenomanian event and Cenomanian–Turonian oceanic anoxic event (OAE 2): Nd isotope evidence. *Geology* **44**, 151–4.